REPUBLIQUE ALGERIENNE DEMOCRATIQUE ET POPULAIRE
الجمهورية الجزائرية الديمقراطية الشعبية

MINISTRY OF HIGHER EDUCATION
AND SCIENTIFIC RESEARCH

HIGHER SCHOOL OF APPLIED SCIENCES
--TLEMCEN--

وزارة التعليم العالي والبحث العلمي

المدرسة العليا في العلوم التطبيقية
-تلمسان-

End of study thesis

For obtaining the Master's degree

Field : **Electrotechnics**
Specialty : **Energy and environment**

Presented by:
TELLAB Souleyman
BOUAZDIA Wail

Theme

Management of a storage system for a grid-connected hybrid photovoltaic/wind system

Publicly defended on 02/07/2023, before the jury composed of:

Mme N. Benahmed	Pr	ESSA. Tlemcen	President
Mr M. Mebrouki	MCA	ESSA. Tlemcen	Thesis Supervisor
Mr A.K. Chemidi	MCA	ESSA. Tlemcen	Examinator 1
Mr A.K. Ghezouani	Doctor	Univ. Bechar	Examinator 2

College year: 2022/2023

Abbreviations

1. DOD : Depth of Discharge
2. SOC : State of Charge
3. AI : Artificial Intelligence
4. ILs : Ionic Liquids
5. LIBs : Lithium-Ion Batteries
6. PV : Photovoltaic
7. Nimh : Nickel-Metal Hydride
8. SOH : State of Health
9. AC : Alternating Current
10. BESS : Battery Energy Storage Systems
11. BMS : Battery Management System
12. DC : Direct Current
13. MPPT : Maximum Power Point Tracking
14. TDT : Total Discharge Time
15. EDC : Energy Discharge Capacity

Abstract

This thesis presents a comprehensive study on the development and optimization of battery management systems for hybrid/wind/photovoltaic systems. The primary objective of this research is to enhance the performance, efficiency, and reliability of energy storage in renewable energy systems. Two battery management strategies, Strategy 2 and Strategy 3, are explored and evaluated using extensive simulation and analysis. The results demonstrate the effectiveness of these strategies in optimizing battery discharge during peak consumption periods and reducing reliance on the grid. Additionally, the integration of wind turbines into the system is investigated to improve power generation and enhance load supply reliability. The proposed battery management strategies not only enable efficient utilization of renewable energy sources but also contribute to prolonged battery lifespan and environmental sustainability. The research findings provide valuable insights and practical guidelines for the design, implementation, and operation of battery systems in hybrid renewable energy systems. This work contributes to the advancement of sustainable energy technologies and serves as a foundation for future research in the field of battery management systems for renewable energy applications.
Keywords: battery management systems, hybrid systems, wind energy, photovoltaic systems, optimization, performance, efficiency, reliability, energy storage, renewable energy, simulation, analysis, battery discharge, grid integration, power generation, load supply, battery lifespan, environmental sustainability, design, implementation, operation, sustainable energy technologies, research.

Résumé

Cette mémoire présente une étude approfondie sur le développement et l'optimisation des systèmes de gestion de batteries pour les systèmes hybrides/éoliens/photovoltaïques. L'objectif principal de cette recherche est d'améliorer les performances, l'efficacité et la fiabilité du stockage d'énergie dans les systèmes d'énergie renouvelable. Deux stratégies de gestion de batteries, Stratégie 2 et Stratégie 3, sont explorées et évaluées à l'aide de simulations et d'analyses approfondies. Les résultats démontrent l'efficacité de ces stratégies dans l'optimisation de la décharge des batteries pendant les périodes de consommation maximale et la réduction de la dépendance au réseau électrique. De plus, l'intégration d'éoliennes dans le système est étudiée afin d'améliorer la production d'énergie et la fiabilité de l'alimentation en charge. Les stratégies de gestion de batteries proposées permettent non seulement une utilisation efficace des sources d'énergie renouvelable, mais contribuent également à prolonger la durée de vie des batteries et à promouvoir la durabilité environnementale. Les résultats de cette recherche fournissent des informations précieuses et des lignes directrices pratiques pour la conception, la mise en œuvre et l'exploitation de systèmes de batteries dans les systèmes d'énergie renouvelable hybrides. Ce travail contribue à l'avancement des technologies d'énergie durable et constitue une base pour des recherches futures dans le domaine des systèmes de gestion de batteries pour les applications d'énergie renouvelable.

Mots clés: systèmes de gestion de batteries, systèmes hybrides, énergie éolienne, systèmes photovoltaïques, optimisation, performances, efficacité, fiabilité, stockage d'énergie, énergie renouvelable, simulations, analyses, décharge de batteries, intégration au réseau, production d'énergie, alimentation en charge, durée de vie des batteries, durabilité environnementale, conception, mise en œuvre, exploitation, technologies d'énergie durable, recherche.

ملخص

تقدم هذه الأطروحة دراسة شاملة حول تطوير وتحسين أنظمة إدارة البطاريات لنظم الطاقة الهجينة / الرياح / الضوئية. الهدف الرئيسي من هذا البحث هو تعزيز الأداء والكفاءة والموثوقية في تخزين الطاقة في نظم الطاقة المتجددة. يتم استكشاف تطبيق استراتيجيتين لإدارة البطاريات في النظام المذكور، وذلك باستخدام محاكاة وتحليل شامل. تظهر النتائج فعالية هذه الاستراتيجيات في تحسين تفريغ البطاريات خلال فترات الاستهلاك الذروة وتقليل الاعتماد على الشبكة. بالإضافة إلى ذلك، يتم استكشاف تكامل أجهزة توربينات الرياح في النظام لتعزيز توليد الطاقة وضمان استدامة توفير الطاقة للأحمال. تضمن استراتيجيات إدارة البطاريات المقترحة ليس فقط استخدام فعّال لمصادر الطاقة المتجددة ، ولكنها أيضًا تعزز عمر البطاريات وتسهم في الاستدامة البيئية. توفر نتائج البحث رؤى قيمة وإرشادات عملية لتصميم وتنفيذ وتشغيل أنظمة البطاريات في نظم الطاقة المتجددة. يسهم هذا العمل في تقدم التقنيات البيئية المستدامة ويشكل أساسًا للبحوث المستقبلية في مجال أنظمة إدارة البطاريات لتطبيقات الطاقة المتجددة.

الكلمات المفتاحية: أنظمة إدارة البطاريات، أنظمة هجينة، طاقة الرياح، أنظمة الطاقة الضوئية، تحسين، أداء، كفاءة، موثوقية، تخزين الطاقة، طاقة متجددة، محاكاة، تحليل، تفريغ البطاريات، الاعتماد على الشبكة، توليد الطاقة، توفير الطاقة، عمر البطاريات، استدامة بيئية، تصميم، تنفيذ، تشغيل، تقنيات الطاقة المستدامة، بحث.

Dedication

To my cherished family,
To my dearest friends,
To my esteemed mentors and advisors,
And to all those who have stood by my side throughout this journey.

Your unwavering support and encouragement have been invaluable
in my pursuit of knowledge and the completion of this thesis.
You have been my guiding lights, offering guidance
and uplifting me during moments of doubt and challenge.

I am deeply grateful for your presence in my life
and for the profound impact you have had on my path.
Your belief in my abilities has fueled my determination,
and I carry your faith and encouragement within me always.

This work is dedicated to each and every one of you
as a tribute to the power of genuine connections,
unyielding support, and shared aspirations.
Thank you for being the pillars of strength in my journey.

With heartfelt appreciation,
TELLAB Souleyman

Dedication

To my family, friends, and mentors,
whose unwavering support and encouragement
have been invaluable throughout my journey.

This work is dedicated to all of you,
as a token of my gratitude
for your belief in me and constant inspiration.

Thank you for always being there
and for making this achievement possible.

With deepest appreciation,
BOUAZDIA Wail

Acknowledgments

We would like to express our sincere appreciation to our supervisor, Mebrouki Mohamed, for his valuable guidance and support throughout this dissertation. We are grateful for his expertise and dedication, which have greatly contributed to the completion of this research. We also extend our thanks to the members of our jury, N. Benahmed, A.K. Chemidi, and A.K. Ghezouani, for their time and insightful feedback. We would like to acknowledge the support and resources provided by the Higher School of Applied Sciences of Tlemcen, which have been instrumental in the completion of this dissertation.

Contents

List of Figures

List of Tables

General introduction

Renewable energy systems, such as hybrid/wind/photovoltaic systems, have gained significant attention in recent years due to their potential to address energy sustainability challenges and reduce greenhouse gas emissions. These systems combine multiple renewable energy sources to ensure a reliable and continuous power supply. However, efficient utilization and management of the generated energy are crucial for the optimal functioning of these systems.

One essential component of such systems is the battery storage system, which plays a vital role in balancing power supply and demand, providing backup power, and improving overall system reliability. The battery management system (BMS) is responsible for monitoring and controlling the operation of the batteries, ensuring their longevity, and maximizing their performance.

The primary objective of this thesis is to develop an advanced battery management system for a hybrid/wind/photovoltaic system with a focus on efficient charge/discharge management and protective measures. The BMS aims to optimize the use of renewable energy sources, enhance system stability, and minimize reliance on the grid. Additionally, it prioritizes the protection of batteries from adverse operating conditions, ensuring their longevity and optimal performance.

The research presented in this thesis involves extensive simulation studies to assess the performance of different battery management strategies. The simulation results provide valuable insights into the behavior of the system under varying conditions, such as different battery temperatures and power demand profiles. These insights aid in the development of effective battery management strategies tailored to the specific requirements of the hybrid/wind/photovoltaic system.

Furthermore, this thesis investigates the impact of integrating wind turbines into the system, not only for power generation but also for load supply. The utilization of wind energy as a supplementary power source enhances system reliability and reduces dependency on the grid during periods of low photovoltaic generation.

The findings of this research contribute to the field of renewable energy systems by providing a comprehensive understanding of battery management in hybrid/wind/photovoltaic systems. The proposed battery management strategies and protective measures enhance the system's overall performance, self-sustainability, and resilience to external factors.

Overall, this thesis aims to bridge the gap between renewable energy generation and efficient utilization by developing an advanced battery management system for a hybrid/wind/photovoltaic system. The research outcomes have the potential to significantly contribute to the development of sustainable energy systems, offering practical solutions for reducing greenhouse gas emissions and promoting a cleaner and more sustainable future.

Chapter 1

An overview of battery storage systems

1.1 Introduction

Batteries are an important energy source for a variety of applications, from portable electronics to renewable energy storage. Understanding battery parameters, protection, conditioning and selection is critical to optimizing battery performance and life. Battery parameters such as capacity, voltage, and self-discharge directly affect efficiency, while protection mechanisms protect against overcharging, deep discharging, and temperature extremes. Factors such as energy requirements, compatibility, size, and cost must be considered when selecting an appropriate battery. In this chapter, we explore these aspects to deepen our understanding and maximize the potential of battery technology. In this chapter, we examine these fundamental concepts, drawing on established research and industry practices to provide valuable insights into the battery world.

1.2 Battery performance characteristics

1.2.1 Battery charging

The charging methods and procedures for batteries display considerable variation. In the forthcoming section on battery charge controllers, we will delve into the diverse methods and associated considerations for battery charging. Additionally, battery manufacturers commonly classify battery charging into three modes: normal or bulk charge, finishing or float charge, and equalizing charge [1].

1.2.1.1 Bulk or normal charge

Bulk or normal charging represents the initial phase of a charging cycle, where the battery is charged at a rate that prevents the cell voltage from exceeding the gassing voltage. This charging mode typically takes place until the state of charge reaches around 80 to 90% [1].

1.2.1.2 Float or finishing charge

Float or finishing charge is employed when the battery is approaching its full charge state. At this stage, a significant portion of the active material within the battery has already been converted to its original form. To prevent overcharging, voltage and/or current regulation is typically necessary to control the amount of charge supplied to the battery. The finishing charge is typically carried out at relatively lower to medium charge rates [1].

1.2.1.3 Equalizing charge

Periodic equalizing or refreshing charges are employed to ensure uniformity among individual cells. An equalizing charge typically involves a current-limited charge that reaches higher voltage limits compared to the finishing or float charge. In the case of batteries that undergo deep discharge on a daily basis, it is recommended to perform an equalizing charge every one or two weeks. For batteries with less severe discharge, equalizing may only be necessary every one or two months. During an equalizing charge, it is typically advised to maintain the charge until the cell voltages and specific gravities remain consistent for a few hours [1].

1.2.2 Battery discharging

1.2.2.1 Depth of discharge(DOD)

Depth of discharge (DOD) is a critical parameter in battery management, representing the percentage of a battery's capacity that has been discharged relative to its total capacity. Monitoring and controlling the DOD is essential to ensure optimal battery performance and lifespan, as discharging a battery beyond its recommended DOD can lead to reduced longevity and diminished overall performance. Assessing the DOD can be achieved through various methods, including voltage measurements or the utilization of strain gauges to track structural changes within the battery. Understanding and managing the DOD is of utmost importance in the context of this thesis, as it directly impacts the efficiency and longevity of battery systems [2, 3].

1.2.2.2 State of charge (SOC)

State of Charge (SoC) is a critical parameter that quantifies the available capacity of a battery, represented as a percentage of its rated capacity. This parameter holds significant importance in battery systems across various applications, including electric vehicles, renewable energy storage, and mobile devices. Accurate measurement and understanding of the SoC enable effective management and utilization of battery systems, ensuring optimal performance and reliable operation. Therefore, within the scope of this thesis, investigating the SoC of batteries is essential for gaining insights into their behavior and efficiency in different practical scenarios [4, 5].

1.2.2.3 Self discharge

Self-discharge refers to the gradual loss of electrical capacity in a battery when it is not in use, resulting from internal electrochemical processes. This phenomenon becomes more pronounced at higher temperatures. To mitigate self-discharge, batteries can be stored at lower temperatures, which helps to reduce the rate of capacity loss over time. Managing self-discharge is crucial in ensuring the long-term effectiveness and performance of batteries [6].

1.2.2.4 Battery lifetime

Battery lifetime is a critical factor in battery management, as batteries inevitably age over time and can lose their capacity to store and deliver energy efficiently. The development of AI-based solutions has shown promise in prolonging battery lifetime, both from a manufacturing and management perspective. However, precise lifetime prediction is challenging due to the simplification of models and measuring errors in testing systems. Empirical-based approaches, such as the physics-chemical, event-oriented, and weighted Ah ageing models, are frequently used for prediction due to their simplicity and smaller workload. These approaches can be valuable tools

for evaluating the economic value of optimization strategies and improving renewable energy quality, but further development is needed to integrate them into power systems [7, 8].

1.2.2.5 Temperature effects

Temperature plays a significant role in the performance of electrochemical cells, including batteries. Typically, a temperature increase of 10°C doubles the rate of electrochemical reactions, leading to battery manufacturers stating that battery life decreases by a factor of two for every 10°C rise in average operating temperature. Higher temperatures can accelerate corrosion of the positive plate grids, resulting in increased gassing and electrolyte loss. On the other hand, lower operating temperatures generally contribute to extended battery life. However, lower temperatures also lead to a significant reduction in capacity, especially in the case of lead-acid batteries. To mitigate the impact of severe temperature variations, batteries are often placed in insulated or temperature-regulated enclosures to minimize the adverse effects on battery performance [1].

1.3 Battery components

1.3.1 Electrodes

The energy storage performance of electrochemical energy storage devices, like lithium-ion batteries and supercapacitors, greatly depends on the electrodes used. Carbon-based materials have long been used as anode materials due to their high chemical stability, conductivity, specific surface area, and capacity retention. However, the low specific capacity and slow lithium diffusion kinetics of graphite have limited its practical application in lithium-ion batteries. Cobalt-based nanomaterials with high theoretical specific capacity have been widely used in lithium-ion battery anodes. In supercapacitors, various materials, including carbonaceous materials, metal compounds, and conducting polymers, have been explored for advanced electrode materials. The design of appropriate nanostructures with sufficient electroactive sites is essential for improving the kinetics of ion and electron transport. Additionally, compounding carbon nanomaterials with cobalt nanomaterials or metal-oxide composites can significantly enhance the electrochemical performance of electrode materials. Composite materials, which exhibit better electrical conductivity, higher cycle ability, and reversibility than single materials, are the result of a synergistic effect between them [9, 10].

1.3.2 Electrolytes

Electrolytes are critical components in electrochemical energy storage systems such as batteries and supercapacitors. In supercapacitors, the electrochemical stability of electrolytes plays a crucial role in determining their working potential. To address the safety concerns associated with current organic electrolytes, ionic liquids (ILs) are being considered as an alternative due to their non-flammability, wide potential windows, and excellent ionic conductivity. IL-based electrolytes have demonstrated attractive energy density and can be utilized in various energy storage systems. While there are currently three types of electrolytes for supercapacitors available commercially, ILs present an opportunity to design efficient and safe electrolytes. They eliminate issues associated with aqueous and organic solvent-based electrolytes, such as narrow operating potential windows, safety concerns, and performance limitations. However, further exploration is needed to realize the full potential of ILs as electrolytes in supercapacitors. To design effective IL-based electrolytes for supercapacitors, factors such as the presence of functional groups in the ILs, their physicochemical and electrochemical properties, and matching

ion size and pore size of the electrolytes and electrode materials need to be considered to achieve desirable capacitances and energy densities [11].

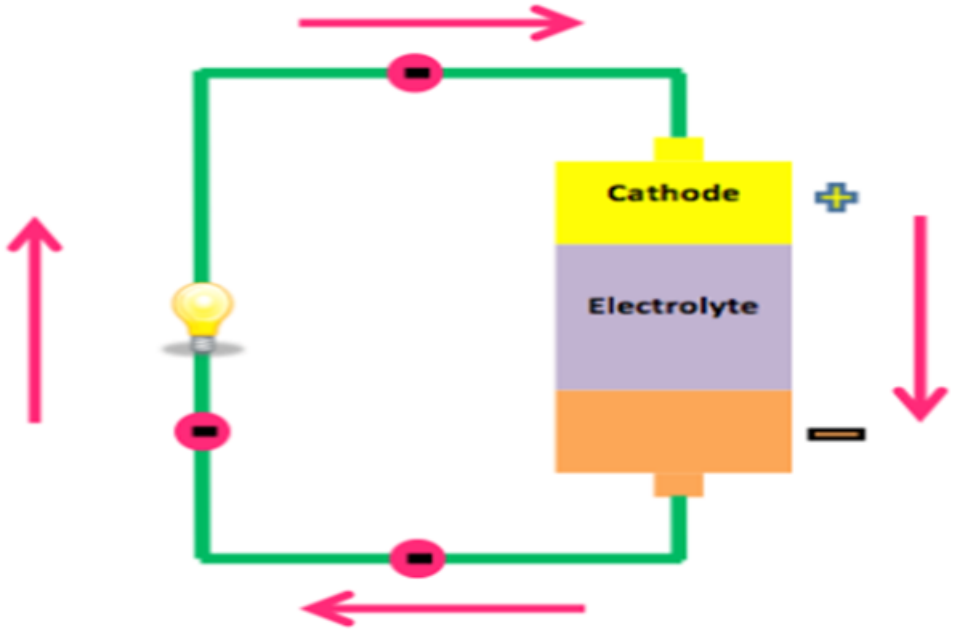

Figure 1.1: Diagram of electrolytes [12].

1.3.3 The separator

The separator is an integral part of lithium-ion batteries (LIBs) that serves as both a physical barrier for the electrode and an electrolyte reservoir for ionic transport. With the increasing demand for high-energy and high-power LIB applications like electric vehicles, portable electronics, and energy storage for power grids, separator technology is an area of significant interest. Separators prevent direct contact between the positive and negative electrodes, while facilitating the movement of lithium ions through the electrolyte. As such, the characteristics of different separators can significantly impact battery performance and safety. High-performance separators require infinite electronic resistance and high ion conductivity, as well as chemical and electrochemical inertness to achieve long-term stability. Researchers have been exploring new separator materials with improved electrical and safety properties, with a focus on preventing shutdown and breakdown. Furthermore, high-temperature-resistant separators are also being developed to meet the evolving needs of LIBs. A comprehensive review of the current development trends and types of high-temperature-resistant separators is provided [13].

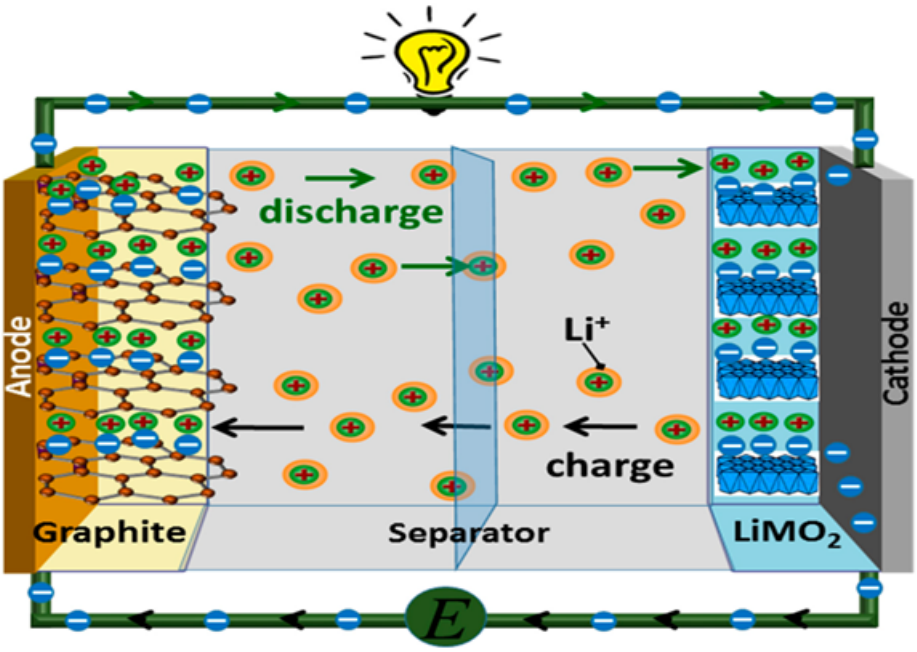

Figure 1.2: Separator [14].

1.3.4 Current collectors

Current collectors play a crucial role in connecting batteries with external circuits, and their properties can significantly affect the capacity, rate capability, and long-term stability of the batteries. The most commonly used current collectors, aluminum and copper foils, have been used since the inception of commercial batteries. However, in order to increase the energy density, the thickness of these current collectors has decreased over the past two decades. To further improve the performance of batteries, researchers have explored alternative materials and structures for current collectors, as well as specific treatments like etching and carbon coating, which can enhance their electrochemical stability and electrical conductivity. These efforts are aimed at developing next-generation lithium-ion batteries with higher capacities and longer service lifetimes [15].

1.3.5 Packaging and casing

In addition to the variety of cell chemistries available, electrochemical cells and batteries are designed in many shapes, sizes, and configurations to meet the diverse performance and design needs of various applications. Proper packaging is an important technological step in creating batteries that are optimal, reliable, and safe for operation. This article examines the current approaches to packaging cells and batteries, including the corresponding materials. The focus is on rechargeable systems for industrial applications such as alkaline systems, lithium-ion, and lead-acid. Four main cell types or shapes can be identified: button, cylindrical, prismatic, and pouch, with varying sizes that may follow international or application-specific standards. However, cell housing, terminals, and safety installations can reduce battery energy density, making the development of lightweight packages a challenging task. Additionally, packaging must meet other requirements, such as mechanical stability and durability, sealing, high packing

efficiency, installation of safety devices, chemical inertness, and cost considerations. Proper cell design is also important for effective thermal management, such as cooling and heating, of battery packs [16].

1.4 Battery protection and regulation

To protect the battery from damage, it is essential to utilize a voltage regulation circuit that prevents overcharging and excessive discharging. Charging the battery too quickly or for prolonged periods can lead to irreversible harm. Overcharging can cause gassing, while excessive discharging can result in plate disintegration. Therefore, maintaining the battery voltage within the specified range using voltage regulating circuits is crucial for its proper operation and longevity [6].

1.4.1 Shunt regulator

The regulator will be connected in parallel with the PV generator to manage the dissipation of excess energy. In the event of regulator failure, battery charging will remain unaffected. Furthermore, during periods of non-regulation, the charging unit experiences no voltage drop, resulting in minimal power consumption [6].

1.4.2 Series regulator

The regulator will be connected in series with the PV generator, ensuring effective regulation of the system. Even during non-regulation periods, the presence of the regulator will result in a voltage drop, leading to some current consumption within the circuit. This ensures continuous monitoring and control of the system, maintaining stability and preventing any potential issues [6].

1.4.3 Electromagnetic series regulator

The battery charging process is halted by an electromechanical device once the voltage reaches the maximum acceptable level. The device automatically resets and recommences charging when the voltage falls back within the specified threshold level. This mechanism ensures that the battery is protected from overcharging while allowing for efficient and safe charging operations [6].

1.4.4 Automatic circuit breaker

In situations of weak sunshine and overloading, it becomes necessary to limit the depth of discharge of the battery by cutting off the load. The regulator is designed to automatically disconnect the load when the voltage reaches a certain threshold level. Once the battery is charged to the required level, the regulator resets itself and allows the load to be connected again. This mechanism ensures that the battery is protected from excessive discharge while providing efficient utilization of available energy resources [6].

1.5 Selecting the right battery

Battery selection involves understanding that there is no one-size-fits-all solution applicable to every situation. The process requires identifying the most important battery metrics and

making trade-offs between them. For example, applications requiring high power necessitate minimizing internal cell resistance, often achieved by increasing electrode surface area. However, this can impact energy density due to the presence of additional inactive components like current collectors and conductive aids. The key is to carefully consider these trade-offs and prioritize the specific requirements of the application when selecting the appropriate battery [17].

1.5.1 Energy and power

Battery runtime is determined by capacity, measured in mAh or Ah, which reflects the discharge current a battery can provide over time. Energy content, calculated by multiplying capacity (Ah) with voltage (V), is essential for comparing batteries of different chemistries. Open-circuit voltage represents the battery's voltage without a load, while capacity and energy depend on the drain rate. Practical batteries achieve a fraction of their theoretical capacity due to inactive materials and kinetic limitations. Battery manufacturers specify capacity based on discharge rate, temperature, and cutoff voltage. High-power batteries offer rapid discharge at high drain rates, with lower energy densities. The analogy of a bucket and spout helps understand the relationship between energy and power. Battery size affects energy, while internal resistance affects power. Battery construction plays a significant role in achieving high power density. Considering these factors is crucial when selecting batteries for specific applications [17].

1.5.2 Voltage

Battery operating voltage is an important factor that is determined by the electrode materials used. There are two main categories to consider: aqueous or water-based batteries and lithium-based chemistries. Aqueous batteries, such as lead-acid, zinc-carbon, and nickel-metal hydride (NiMH), utilize water-based electrolytes and typically have nominal voltages ranging from 1.2 to 2 V. In contrast, lithium-based batteries use organic electrolytes and exhibit nominal voltages of 3.2 to 4 V for both primary and secondary variants [17].
Considering the voltage requirements of electronic components, many devices operate at a minimum voltage of 3 V. The higher operating voltage of lithium-based chemistries provides an advantage as it enables the use of a single cell, eliminating the need to combine two or three aqueous-based cells in series to achieve the desired voltage level. This offers greater convenience and efficiency in certain applications, simplifying battery configurations and improving overall performance [17].

1.5.3 Temperature range

The selection of battery chemistry is a critical factor in determining the suitable temperature range for a given application. Different battery types exhibit varying temperature dependencies. For example, zinc-carbon cells with aqueous electrolytes are not recommended for use below 0 C , while alkaline cells also experience reduced capacity at low temperatures. On the other hand, lithium primary batteries with organic electrolytes can operate at temperatures as low as -40 C , albeit with decreased performance [17].
In rechargeable applications, such as lithium-ion batteries, the charging process is most efficient within a specific temperature range, typically around 20-45 C. Charging at temperatures outside this range requires adjustments in current and voltage, leading to longer charging times. Cold temperatures, below 5-10 C , may necessitate a trickle charge to prevent issues like lithium dendritic plating, which can lead to thermal runaway and safety hazards. It is crucial to avoid overcharging, charging at extreme temperatures, or exposing the battery to short-circuits caused by contaminants to mitigate the risk of battery malfunction or potential incidents [17].

1.5.4 Cost

In certain situations, the selection of a battery may require prioritizing cost considerations over superior performance characteristics. This scenario is particularly relevant in cost-sensitive applications, especially those involving high-volume disposable devices [17].

1.6 State of health (SOH)

The state of health (SOH) of a battery refers to its overall capacity or the amount of charge, measured in ampere-hours, that it would deliver if discharged completely from a fully charged state. It can be standardized as the ratio between the measured capacity and the initial capacity (or nominal capacity) of the battery [18].

1.6.1 Importance of battery health assessment

Assessing the health of batteries is crucial for ensuring the optimal performance and longevity of large battery packs while effectively managing battery degradation. The state of health (SOH) of a battery pack is a fundamental parameter that plays a significant role in its proper operation. Various methods, including the defining method, internal resistance method, AC impedance, voltage curve method, model method, and emerging techniques, can be employed to estimate the SOH of batteries. Accurately determining the SOH is essential for ensuring battery safety, managing degradation, and maintaining optimal performance throughout its operational lifespan [19–21].

1.6.2 Factors affecting battery state of health

The state of health (SOH) of a battery is primarily determined by the degradation of its capacity and the increase in internal resistance. Additionally, various factors impact the overall health and functionality of the battery, including the choice of electrode materials, operating conditions, battery temperature, charging and discharging methods, and state of charge. Extreme temperatures and abnormal charging/discharging conditions can accelerate battery aging and potentially lead to battery failure. As a battery ages, the rate at which its voltage decreases during discharging tends to increase, while the speed at which terminal voltage increases during constant current charging also rises with deteriorating health. The time required for constant current charging operation decreases as the battery ages, and the rate at which the battery current decreases during constant voltage charging increases over time. Low temperatures can restrict the attenuation morphology of power batteries, while high temperatures can weaken the solid-electrolyte interface. Different battery types exhibit specific patterns of capacity reduction. Hence, it is crucial to consider these factors in battery health management research, which involves identifying relevant parameters and employing accurate equivalent models [22–25].

1.7 Environmental impact

1.7.1 Life cycle assessment of batteries

The environmental impact of batteries must be carefully considered throughout their entire life cycle, from materials extraction to end-of-life disposal. The mining of minerals used in battery production can have significant environmental impacts, including habitat destruction and pollution. During the manufacturing stage, battery component production consumes energy and water and generates waste and emissions. Additionally, the use phase of batteries involves

energy consumption and greenhouse gas emissions, which contribute to climate change. Finally, the end-of-life disposal of batteries can lead to environmental pollution and the release of toxic substances into the environment. In order to minimize the environmental impact of batteries, strategies should be developed that incorporate more sustainable materials, efficient manufacturing processes, improved battery performance and longevity through AI-based solutions, and non-disruptive diagnostic techniques for monitoring battery health. Implementing these strategies can promote battery sustainability and help reduce their impact on the environment [26,27]

1.7.2 Comparison of environmental impact of different battery technologies

The environmental impact of batteries varies depending on their chemistry and life cycle stages. Lithium-ion batteries (LIBs) are widely used due to their high specific capacity, long cycle life, and lack of memory effects, but their production and disposal can have significant environmental impacts. In response, alternative battery chemistries such as sodium-ion batteries and solid-state batteries have been proposed as more environmentally friendly options. While these alternatives have promising features, they are still in the early stages of development and have not yet been widely adopted. To minimize the environmental impact of batteries, it is crucial to continue researching and developing more sustainable battery chemistries that incorporate efficient manufacturing processes and reduce environmental pollution and toxic substances throughout their life cycle [26, 28]

1.7.3 Strategies for minimizing the environmental impact of battery energy storage systems

As the demand for renewable energy sources grows, battery energy storage systems (BESS) have become essential. However, it is crucial to minimize the environmental impact of BESS throughout their life cycle. One approach to achieve this is through the development of advanced and eco-friendly materials for battery components, such as anode, cathode, and separator/electrolyte. Another strategy is to use AI-based manufacturing and management solutions to improve battery health and extend battery life, thus reducing waste and the need for frequent battery replacements. Efficient recycling of waste batteries is also crucial in reducing environmental impact. Information management and analysis of battery efficiency data can help classify waste batteries and evaluate the benefits of each different waste battery at the use level, facilitating their recycling. Additionally, alternative battery chemistries, such as sodium-ion batteries and solid-state batteries, can reduce the environmental impact of BESS by utilizing low-cost and abundant materials while improving safety and minimizing the risk of leakage [26, 29].

1.8 Conclusion

Finally, this chapter emphasized the importance of understanding battery parameters, protection mechanisms, selection criteria, and health assessment. By considering these factors, users can optimize battery performance, ensure safe operation, and extend battery life. Choosing the right battery for a particular application is important considering performance requirements, compatibility, and other factors. By monitoring battery health, you can perform timely maintenance and eliminate deterioration. Overall, this knowledge is essential for maximizing battery efficiency and reliability in a variety of situations.

Bibliography

[1] Dunlop, J.P. (January 15, 1997). *Batteries and Charge Control in Stand Alone Photovoltaic Systems: Fundamentals and Application*. Florida Solar Energy Center.

[2] Hendricks, C. et al. (2022). *Lithium-Ion Battery Strain Gauge Monitoring and Depth of Discharge Estimation*. Semantic Scholar. DOI: 10.1115/1.4054340.

[3] Chaba, N., Neramitthagapong, S., Neramitthagapong, A., EuA-Anant, N., & Theerakulpisut, S. (2021). Effect of Depth of Discharge on the Performance of Zn-Mn and Zn-Ni Battery. *Journal of the Japan Institute of Energy*, *100*(8), 144–151. The Japan Institute of Energy. https://doi.org/10.3775/jie.100.144

[4] Murnane, M., Ghazel, A., Omar, N., O'Sullivan, J. (2017). A Closer look at state of charge (SOC) and state of health (SOH) estimation techniques for batteries. *Semantic Scholar*. https://www.semanticscholar.org/paper/A-Closer-Look-at-State-of-Charge-(-SOC-)-and-State-Murnane-Ghazel/964c93c82bf2ee272c6491b3cb85a06529e935d2#citing-papers

[5] Espedal, I. B., Jinasena, A., Burheim, O. S., & Lamb, J. J. (2021). Current Trends for State-of-Charge (SoC) Estimation in Lithium-Ion Battery Electric Vehicles. *Energies*, 14(11), 3284. doi:10.3390/en14113284

[6] Manimekalai, P., Harikumar, R., & Raghavan, S. (2013). An Overview of Batteries for Photovoltaic (PV) Systems. *International Journal of Computer Applications*, 82(12), 28–32. doi:10.5120/14170-2299

[7] Zhang, P., Liang, J., & Zhang, F. (2017). An Overview of Different Approaches for Battery Lifetime Prediction. *IOP Conference Series: Materials Science and Engineering*, 199, 012134. doi:10.1088/1757-899x/199/1/012134

[8] Lui, K., et al. (2022). Towards Long Lifetime Battery: AI-Based Manufacturing and Management. *Semantic Scholar*. Retrieved from https://www.semanticscholar.org/.

[9] Chen, H., et al. (2022). A Review of Cobalt-Containing Nanomaterials, Carbon Nanomaterials and Their Composites in Preparation Methods and Application. *Nanomaterials*, 12(12). doi:10.3390/nano12122042.

[10] Wu, Z., et al. (2017). Materials Design and System Construction for Conventional and New-Concept Supercapacitors. *Advanced Science*. doi:10.1002/advs.201600382.

[11] Pan, S., et al. (2020). Recognition of Ionic Liquids as High-Voltage Electrolytes for Supercapacitors. *Frontiers in Chemistry*. doi:10.3389/fchem.2020.00261.

[12] Richard. (September 19, 2016). What are Electrodes & What Do They Do? *UPS Battery Center Blog*. Retrieved from *https://www.upsbatterycenter.com/blog/electrodes-what-they-do/*

[13] Li, A., et al. (2021). A Review on Lithium-Ion Battery Separators towards Enhanced Safety Performances and Modelling Approaches. *Molecules*, 26(2), 478. doi:10.3390/molecules26020478.

[14] Madian, M., Eychmüller, A., Giebeler, L. (2018). Current Advances in TiO2-Based Nanostructure Electrodes for High Performance Lithium-Ion Batteries. *Batteries*, 4(1), 7. doi:10.3390/batteries4010007.

[15] Zhu, P., et al. (2021). A Review of Current Collectors for Lithium-Ion Batteries. *Journal of Power Sources*, 487, 229321. https://doi.org/10.1016/j.jpowsour.2020.229321.

[16] Herrmann, M. (2014). Packaging – Materials Review. *AIP Conference Proceedings*, 1597(1). https://doi.org/10.1063/1.4878483.

[17] Challa, V. (April 27, 2022). Selecting the Right Battery for Your Application, Part 1: Important Battery Metrics. *ANSYS Blog*. Retrieved from https://www.ansys.com/blog/important-battery-metrics.

[18] Delaille, M. A. (October 26, 2006). Développement de méthodes d'évaluation de l'état de charge et de l'état de santé des batteries utilisées dans les systèmes photovoltaïques. Doctoral thesis.

[19] Dubarry, M., Baure, G.,Anseán, D. (2020). Perspective on State-of-Health Determination in Lithium-Ion Batteries. Journal of Electrochemical Energy Conversion and Storage, 17(4), ASME International. https://doi.org/10.1115/1.4045008.

[20] Liu, P., et al. (2018). Progress of State of Health Evaluation Methods for Lithium-Ion Power Battery. IOP Conference Series: Materials Science and Engineering, 452(3). https://doi.org/10.1088/1757-899X/452/3/032033.

[21] Alvarez-Monteserin, I., & Sanz-Bobi, M. A. (2022). An Online Fade Capacity Estimation of Lithium-Ion Battery Using a New Health Indicator Based Only on a Short Period of the Charging Voltage Profile. IEEE Access, 10, 11138–11146. https://doi.org/10.1109/access.2022.3143107.

[22] Balagopal, B., & Chow, M.-Y. (2015). The state of the art approaches to estimate the state of health (SOH) and state of function (SOF) of lithium Ion batteries. In 2015 IEEE 13th International Conference on Industrial Informatics (INDIN). IEEE. https://doi.org/10.1109/indin.2015.7281923.

[23] Li, X., et al. (2021). Research on capacity degradation and aging state estimation of lithium-ion battery. Journal of Physics: Conference Series. https://doi.org/10.1088/1742-6596/2011/1/012082.

[24] Xia, Z. (2021). Lithium-Ion Battery ageing behavior pattern characterization and state-of-health estimation using data-driven method. IEEE Access. https://doi.org/10.1109/ACCESS.2021.3092743.

[25] Li, D. (2021). Influence factors and identification of state-of-health for traction battery. IOP Conference Series: Materials Science and Engineering. https://doi.org/10.1088/1757-899X/1043/5/052037.

[26] Barbosa, J.C., Gonçalves, R., Costa, C.M., Lanceros-Mendez, S. (2021). Recent advances on materials for lithium-ion batteries. Energies, 14, 3145. https://doi.org/10.3390/en14113145.

[27] Branco, H., Castro, R., & Lopes, A. (2018). Battery energy storage systems as a way to integrate renewable energy in small isolated power systems. Energy for Sustainable Development, 43, 90–99. doi:10.1016/j.esd.2018.01.003

[28] Xu, C., Dai, Q., Gaines, L., Hu, M., Tukker, A., & Steubing, B. (2020). Future material demand for automotive lithium-based batteries. Communications Materials, 1(1). doi:10.1038/s43246-020-00095-x

[29] Liu, K. L., Wei, Z. B., Zhang, C. H., Shang, Y. L., Teodorescu, R., Han, Q.-L. (2022). Towards long lifetime battery: AI-based manufacturing and management. IEEE/CAA Journal of Automatica Sinica, 9(7), 1139–1165. doi:10.1109/JAS.2022.105599.

Chapter 2

Empowering battery storage: smart charging, discharging, and modeling

2.1 Introduction

The integration of renewable energy into the modern grid underscores the increasing importance of battery energy storage systems (BESS) for maintaining supply balance and improving grid reliability. Among various technologies, lithium-ion batteries have emerged as a promising option for grid integration and renewable energy storage. However, it is crucial to recognize that the cost of lithium-ion batteries remains relatively high. In this dissertation, we focus on reviewing and evaluating the current state of lead-acid battery technology in managing network connectivity, encompassing the battery build model and the physical structure of a battery management system (BMS). We also delve into the combination of electricity market services, global utility-regulated battery storage facilities, and the challenges associated with implementing and managing network connectivity using lead-acid batteries. The increasing number of BESS installations worldwide highlights the potential of lead-acid batteries to offer a range of grid support services. Additionally, we conduct a comparative analysis of different battery models and assess the impact of BESS on power systems and microgrids. Our findings indicate that lead-acid batteries are well-suited for grid integration, contributing to the reduction of renewable energy volatility. However, it is important to note that the cost of lead-acid batteries remains a significant obstacle for their widespread adoption in renewable energy integration. [1] [2] [3].

2.2 Exploring the energy system

The diagram (figure 2.1) illustrates a hybrid wind and photovoltaic system with grid-connected battery storage, showcasing an efficient configuration for integrating renewable energy sources into the power grid. In our hybrid energy system, we have opted a parallel architecture consisting of AC and DC buses. The surplus power generated by the photovoltaic panels is utilized for charging the batteries through a DC to DC converter. The power generated by the wind turbines directly powers the load, reducing reliance on the grid. Both the power from the photovoltaic panels and the batteries pass through a DC to AC converter before being utilized by the load. In instances of overall production surplus, excess energy can be sold back to the grid. This configuration enhances energy independence, promotes renewable energy utilization, and facilitates grid interaction for optimal energy management. This comprehensive system configuration optimizes renewable energy generation, storage, and utilization, offering a sustainable and environmentally friendly solution for the power grid.

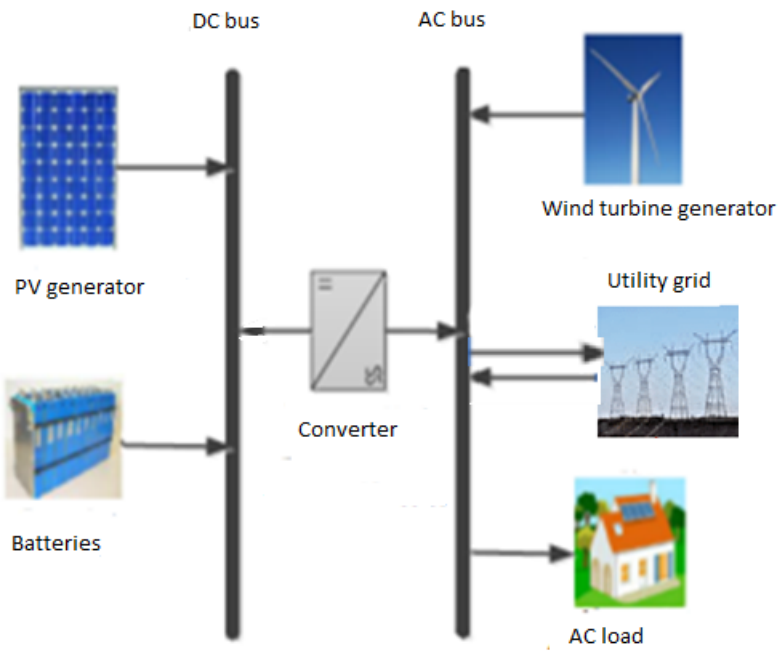

Figure 2.1: Configuration of a hybrid wind and photovoltaic system with grid-connected battery storage [4].

2.3 Modeling of the photovoltaic generator

A model has been proposed to calculate the alternating power P_{AC}, which is used to determine the energy produced by the photovoltaic system. The model enables the calculation of the photovoltaic energy production converted into alternating current, P_{AC}, according to the following formula [5, 6]:

$$P_{AC} = P_{\mathrm{n,pv}} \frac{G}{G_{\mathrm{STC}}} \eta_{\mathrm{mix}} \eta_{\mathrm{therm}} \eta_{\mathrm{DC/AC}} \tag{2.1}$$

In the provided equation, the following parameters and efficiencies are defined:

- G represents solar irradiance, measured in $\mathrm{W/m^2}$.
- G_{STC} corresponds to irradiance under standard test conditions.
- $P_{\mathrm{n,pv}}$ denotes the nominal power of the PV generator.
- η_{mix} represents the efficiency associated with various technical or environmental factors leading to losses.
- η_{therm} refers to the efficiency of thermal losses in the photovoltaic generator.
- $\eta_{\mathrm{DC/AC}}$ represents the efficiency of the DC/AC conversion process.

Alternatively, the expression for the efficiency η_{mix} is given by [6]:

$$\eta_{mix} = \eta_{\mathrm{dirt}} \eta_{\mathrm{rfl}} \eta_{\mathrm{mis}} \eta_{\mathrm{MPPT}} \eta_{\mathrm{cabl}} \eta_{\mathrm{shad}} \tag{2.2}$$

- η_{dirt} is a parameter that quantifies losses resulting from dust accumulation on the panel.
- η_{rfl} has a relationship with losses due to reflection on the glass of the photovoltaic panel.

- η_{mis} is an estimation of mismatch losses that lead to the degradation of the I-V characteristics of PV modules.
- η_{MPPT} estimates losses caused by the tracker's inability to accurately determine the maximum power point.
- η_{cabl} is caused by joule losses in the cables used.
- η_{shad} quantifies shading losses in a photovoltaic system, calculated as the ratio between the power generated by the PV panel under shading conditions during various seasons at a specific installation site and the power generated without shading. It is important to measure both power values under identical conditions in order to accurately assess the impact of shading on system performance.

The efficiency related to thermal losses in the photovoltaic generator, η_{therm}, is directly influenced by the cell temperature, T_c, which can be determined using the following formula. Additionally, to estimate the temperature losses, the PV cell temperature, T_c, is calculated at each time step based on the measured air temperature, Ta, using the following equation [6]:

$$T_C = T_a + \frac{(NOCT - 20)}{G_{\text{NOCT}}} G \tag{2.3}$$

The parameter NOCT signifies the standard operating temperature of the cells, which is commonly provided by PV module manufacturers. In this study, it is assumed to be 45 C. G_{NOCT} represents the solar irradiation level experienced under NOCT conditions, amounting to 800 W/m^2. The following formula is used to calculate the efficiency of thermal losses in the photovoltaic generator [6]:

$$\eta_{\text{therm}} = 1 - \gamma_{th}(T_{\text{c}} - T_{\text{STC}}) \tag{2.4}$$

Where T_{STC} and γ_{th} The power temperature coefficient of the PV generator. calculated in (% / C).

2.4 Modeling of the wind turbine generator

The power output of a wind turbine is directly influenced by the wind speed it experiences. When the wind speed surpasses the cut-in velocity (V_{ci}), the power generated by the turbine increases proportionally with the wind speed. Once the wind speed exceeds the rated velocity (V_r), the power output of the turbine remains constant and equals the rated power (P_r). However, if the wind speed exceeds the cut-out value (V_{co}), the turbine automatically shuts down as a protective measure, resulting in zero power generation. [7].

$$p_{WT} = \begin{cases} 0 & V(t) < V_{\text{ci}} \text{ or } V(t) > V_{\text{co}} \\ P_r \cdot \dfrac{V(t) - V_{ci}}{V_r - V_{ci}} & V_{ci} < V(t) < V_r \\ P_r & V_r \leq V(t) \leq V_{co} \end{cases} \tag{2.5}$$

2.5 Modeling of the storage system

In this study, a simplified battery management model is employed to analyze the dynamics of battery state of charge (SOC) over time. The charging and discharging voltages proposed by J.B Copetti et al are utilized as reference values. The research is based on practical experiments conducted on various lead-acid batteries connected to a photovoltaic generator. Through

mathematical analysis, the model determines the battery voltage variation and the behavior of internal resistance during charge/discharge cycles under different temperatures and currents, denoted as I(C_n). For instance, I(C_{10}) represents the current delivered by a battery with a nominal capacity of C_{10} during a 10-hour discharge. The relationship between battery cell voltage (V_d), current (I), state of charge (SOC), and cell temperature during discharge is described by a specific equation [3, 8]:

$$V_d = [2.085 - 0.12(1 - SOC)] - \frac{I}{C_{10}} \left(\frac{4}{1 + I^{1.3}} + \frac{0.27}{SOC^{1.5}} + 0.02 \right) (1 - 0.007\Delta T) \tag{2.6}$$

The first term in the equation represents the voltage variation related to the state of charge (SOC) and electrolyte concentration, while the second term accounts for the variation caused by changes in internal resistance. Through specific tests conducted, a relationship between internal resistance and temperature, state of charge, and current during charge and discharge was established. The battery behavior was considered as a series of steady states, ignoring transient effects, due to the utilization of specific current rates. In the Equation , the internal resistance is represented as the sum of series resistances associated with different phenomena. The temperature variation, denoted as ΔT, is calculated as the difference between the actual temperature (T) and the reference temperature (ref), which is set at 25 C [8]. The state of charge (SOC) is a measure that indicates the amount of electric charge stored in the cell at a specific moment. It is defined as follows [8]:

$$SOC(i) = SOC(i - 1) - \frac{Q}{C} \qquad \text{for} \quad P_{\text{bat}} > 0 \tag{2.7}$$

The depth of discharge (DOD) or fraction of discharge is represented by the ratio of the charge delivered at the time of interest ($Q = It$) to the battery capacity (C). Mathematically, it can be expressed as $DOD = 1 - SOC$. The total amount of useful charge available during discharge is limited by the current rate and temperature, as described by the capacity equation. This equation is normalized with respect to the discharge current that corresponds to the rated capacity (C_{10}), which is denoted as I_{10} [8].

$$\frac{C}{C_{10}} = \frac{1.67}{1 + 0.67(I/I_{10})^{0.9}} (1 + 0.005\Delta T) \tag{2.8}$$

where C is normalized with respect to the nominal capacity C_{10}. It should be noted that the discharge current is defined as follows [8]:

$$I = \frac{P_{\text{l}} - P_{\text{WT}} - P_{\text{load, max}}}{\eta_{\text{inv}} V_{\text{l, nominal}}} \tag{2.9}$$

Where P_{l} is the power demanded by the load ,$P_{\text{load, max}}$ A lower limit of the charging power above which the batteries start to discharge. ηinv The efficiency of the inverter $V_{\text{l, nominal}}$ The nominal voltage of the load (AC), The discharge power of the batteries is thus written as [8]:

$$P_{\text{d,bat}} = V_d \cdot I_d \cdot N_{\text{bat,s}} \cdot N_{\text{cell}} \tag{2.10}$$

. V_d represents the voltage at which a cell is discharged.

. I_d is the discharge current.

. $N_{\text{bat,s}}$ is the number of batteries in a branch.

. N_{cell} is the number of cells in a battery.

Furthermore, the equation below represents the charging voltage of a cell [8]:

$$V_c = [2 + 0.16\,SOC)] + \frac{I}{C_{10}}\left(\frac{6}{1 + I^{0.86}} + \frac{0.48}{(1 - SOC)^{1.2}} + 0.036\right)(1 - 0.025\Delta T) \tag{2.11}$$

Determining the state of charge during battery charging is much more complex compared to discharging. We have proposed a function that describes the evolution of the battery state of charge (SOC) during the charging process [8].

$$SOC(i) = SOC(i-1) + \frac{\eta_{\text{ch}} I_c t}{C_{10} N_{\text{par}}} \quad \text{for} \quad P_{\text{bat}} < 0 \tag{2.12}$$

. η_{ch} is the charging efficiency of the batteries.

. I_c is the charging current.

. C_{10} is the nominal capacity of the batteries.

. N_{par} is the number of parallel branches in the battery bank.

In this scenario, the power used for charging the batteries is denoted as $P_{\text{c,bat}}$ [8]:

$$P_{\text{c,bat}} = \eta_{\text{ch}} \cdot V_c \cdot I_c \cdot N_{\text{bat,s}} \cdot N_{\text{cell}} \tag{2.13}$$

In the given context, η_{ch} represents the efficiency of battery charging, V_c corresponds to the voltage at which the battery cells are charged, I_c refers to the charging current, $N_{\text{bat,s}}$ denotes the number of batteries in a series configuration, and N_{cell} indicates the number of cells within a single battery.
Furthermore, we can express the charging efficiency through the following equation [8]:

$$\eta_{\text{cc}} = 1 - \exp[\frac{a}{(I/I_{10}) + b}(SOC - 1)] \tag{2.14}$$

The parameters a and b are associated with the battery type. Models used to estimate the state of health (SOH) of a battery rely on continuous measurements of parameters such as voltage, current, and temperature. Consequently, the calculation of SOH cannot rely solely on simulations and necessitates experimental studies.

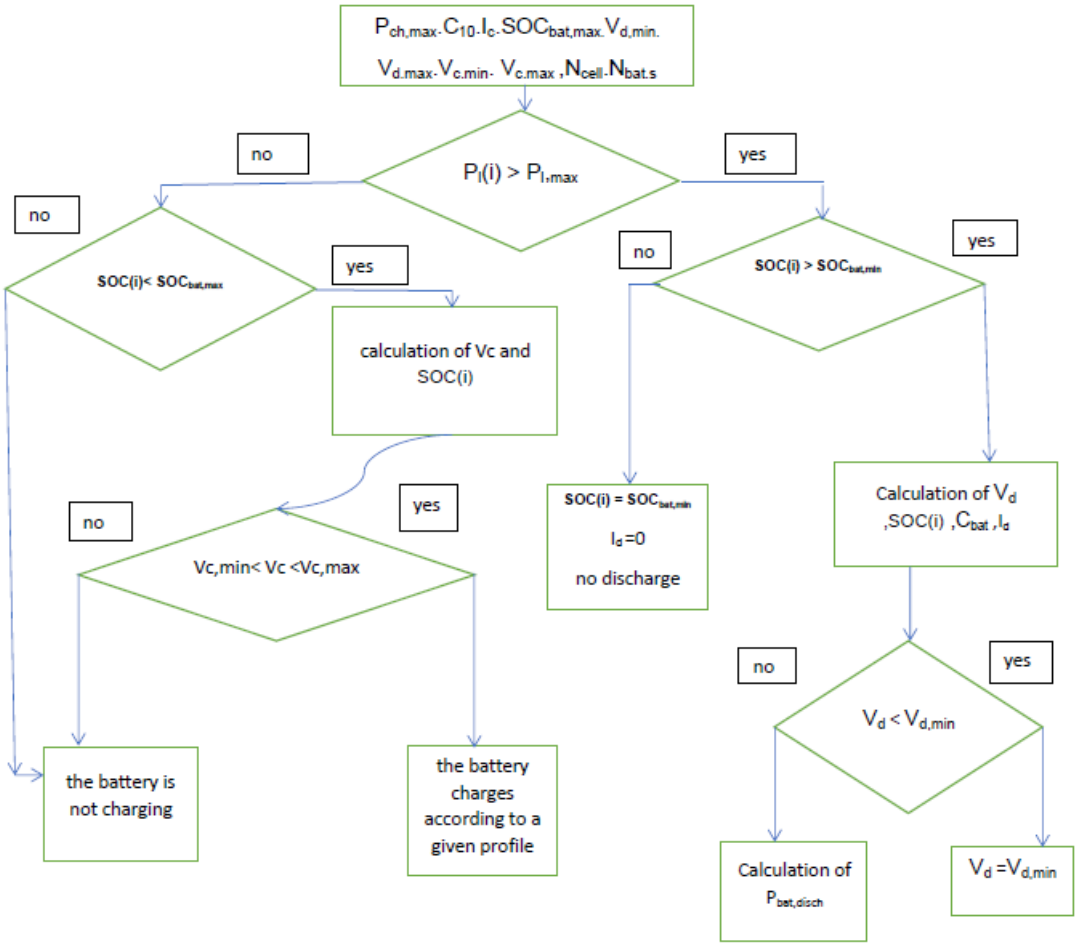

Figure 2.2: Charge and discharge flowchart of the batteries [10].

2.6 Charging methods

2.6.1 Constant voltage charging

The standard method for charging lead-acid batteries is widely employed due to its ability to reduce charging time and enhance capacity by up to 20%. However, it is important to note that this method incurs a reduction in efficiency of approximately 10%. During the charging process, a constant charging voltage is maintained, while the charging current starts at a high value when the battery is in a discharged state. As the battery begins to charge, the current gradually decreases as the battery's charge level increases [11]. Charging at a constant voltage offers several advantages. Firstly, it accommodates cells with varying capacities and allows for the charging of cells with different degrees of discharge. The initial high charging current, which is of a relatively short duration, poses no harm to the cell. As the charge progresses and the battery voltage approaches the supply circuit voltage, the charging current gradually diminishes until it reaches almost zero at the end of the charge. This behavior is a result of the battery voltage nearing equilibrium with the supply circuit voltage [11].

2.6.2 Constant current charging

In this charging method, batteries are arranged in series to create smaller groups. Each group is then charged from the DC supply mains through-loading rheostats. The charging process within each group is contingent upon the charging circuit voltage, which must not fall below

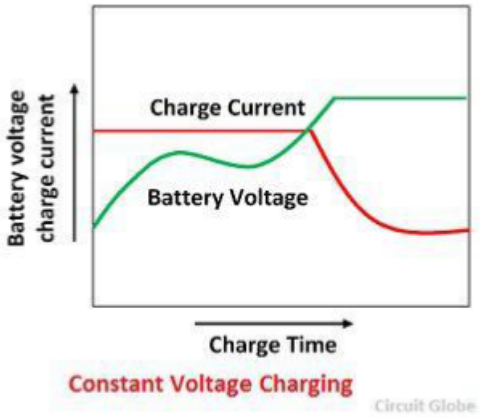

Figure 2.3: Constant voltage method [11].

2.7 V per cell [11].
To maintain a constant charging current throughout the process, the circuit's resistance is gradually reduced as the battery voltage increases. To prevent excessive gassing or overheating, the charging process may be divided into two steps. Initially, a higher current is applied for the initial charging phase, followed by a lower current for the finishing stage. This multi-step approach ensures safe and efficient charging of the batteries [11]. In this particular charging

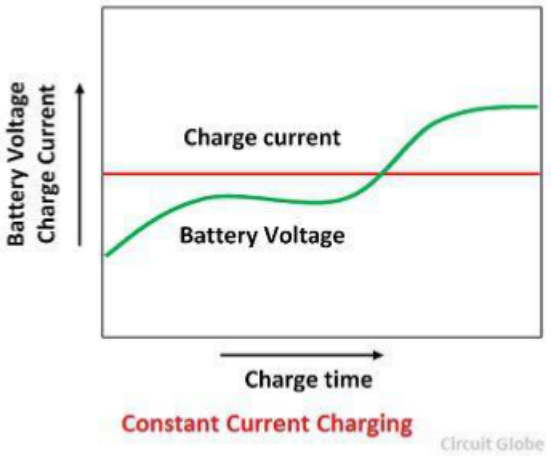

Figure 2.4: Constant current method [11].

method, the charging current is maintained at approximately one-eighth of the batteries ampere ratings. Any excess voltage from the supply circuit is dissipated through the use of a series resistance. It is essential to ensure that the battery groups are connected in a way that minimizes energy loss through the series resistance [11].
The series resistance selected should have a current carrying capacity that matches or exceeds the required charging current. Failure to meet this criterion may result in overheating and potential damage to the resistance component [11].
When selecting the group of batteries for charging, it is crucial to ensure that they have identical capacities. In the event of varying capacities within a battery group, adjustments should be made based on the battery with the lowest power capacity to ensure consistent charging performance and optimal battery health [11].

2.6.3 Mixed constant current / constant voltage charging method

The constant voltage and constant current charging methods have distinct advantages and disadvantages. To address their limitations, a proposed solution is the constant current/constant voltage charging method. This method offers significant benefits, including reduced charging time and the ability to self-regulate current without risking battery overcharging. In this approach, the initial stage employs the constant current mode, allowing the battery to quickly replenish energy by accepting higher current when it is at a low state of charge. Once the battery voltage reaches a predetermined level, the charger seamlessly transitions to the constant voltage mode, known as the equalization mode. During this phase, charging is maintained at a constant voltage to ensure efficient battery balancing. Upon reaching full charge, the charger automatically switches to the floating mode, maintaining the battery at an optimal charge level. This proposed mixed constant current/constant voltage charging method presents an innovative and effective approach to overcome the limitations of traditional methods, contributing to the advancement of efficient and sustainable energy storage systems [11].

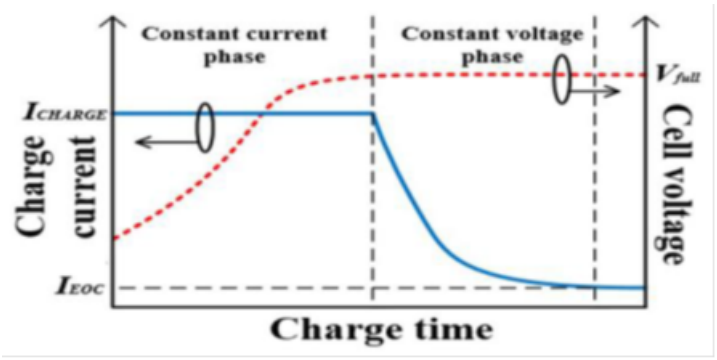

Figure 2.5: Mixed constant current / constant voltage charging method [11].

2.7 Intelligent energy storage management and energy balance

We present a Battery Management System (BMS) that continuously and periodically establishes a strategy to minimize reliance on the grid. This strategy is selected twice within a 24-hour timeframe to meet energy demands during peak consumption periods. Our BMS divides the day into three distinct time periods. The first period spans from midnight to 6:00 AM, followed by the second period from 6:00 AM to 6:00 PM, during which photovoltaic energy generation occurs. The final period extends from 6:00 PM to midnight [10].
At 6:00 PM, the BMS updates the strategy as the electric energy generated by the photovoltaic system becomes unavailable. The BMS then calculates the stored capacity of the batteries to be utilized in the subsequent period. In this study, the batteries are exclusively charged from 6:00 AM to 6:00 PM when photovoltaic energy is abundant. Consequently, the batteries do not undergo charging from 6:00 PM to 6:00 AM. By comparing the estimated energy production and consumption, the BMS provides a temporary energy balance for a day based on the expected electrical load profile [10].

2.8 Total discharge time:

Determining the total discharge time (TDT) is the first step in battery management. At 6:00 PM, the system considers two factors: the forecasted photovoltaic production for the following

day and the load that needs to be supplied from 6:00 AM to 6:00 PM. By comparing these two data sets, a balance is established. If the expected production exceeds the consumption, the batteries will discharge for a total of 12 hours. Throughout the day (6:00 AM to 6:00 PM), any renewable energy generated will be used to power the load, with any excess energy being stored in the batteries or injected into the grid [8].
Conversely, if the projected consumption exceeds the photovoltaic production for the current day, meaning that the production cannot meet the load requirements, the stored energy will be utilized to minimize the consumption over the next two nights (storage management plans are made two days in advance). In this case, the total discharge time (TDT) will be set to 36 hours [8].

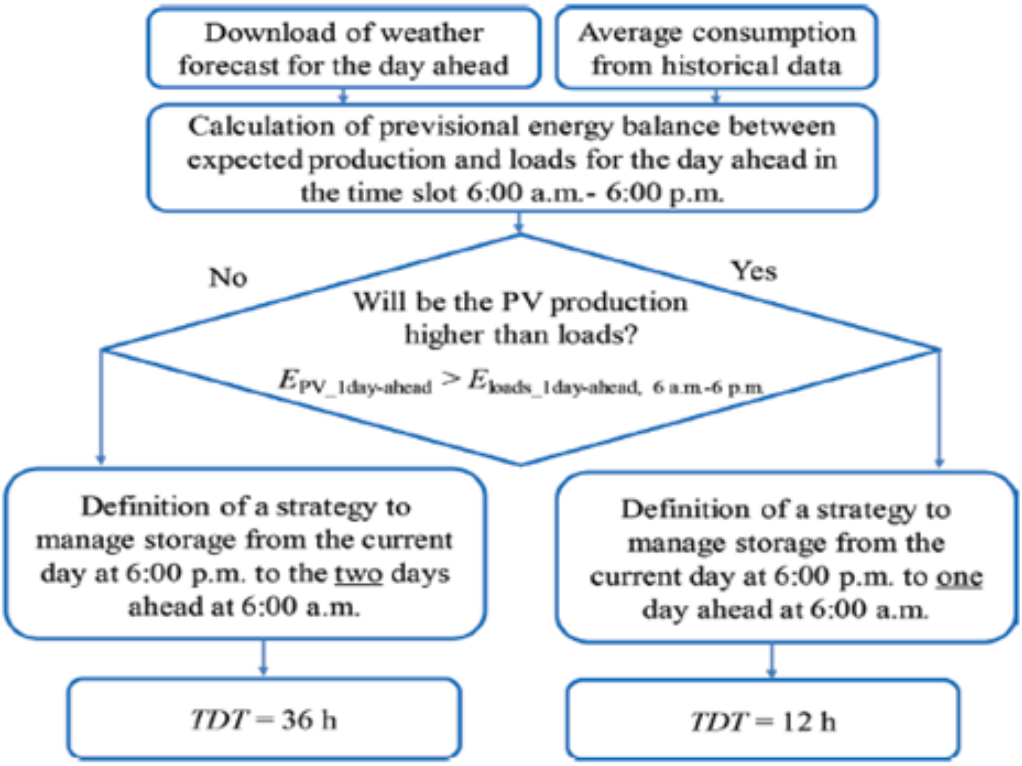

Figure 2.6: Choice of total discharge time TDT [3].

2.9 Choice of battery management strategy

After determining the TDT, the next step is to select the strategy for managing battery charge/discharge. At 6:00 PM, the Battery Management System (BMS) evaluates the state of charge of the storage system based on the batteries' nominal capacity and the calculation of the Energy Discharge Capacity. By determining the available energy stored in the batteries, the BMS accurately determines the energy that can be supplied to the load (battery discharge energy). The BMS also estimates the expected consumption during the discharge period and the projected energy production for the following day [8].
Subsequently, the BMS combines the two energy values: the energy stored in the batteries and the energy generated by the PV system. If the calculated value is lower than the estimated consumption, indicating a deficit due to high load [8]. If the load exceeds the total energy available from both generation and storage, a strategy known as peak shaving (BMS2) is employed. On the other hand, if the load is lower than the combined energy, an alternative approach

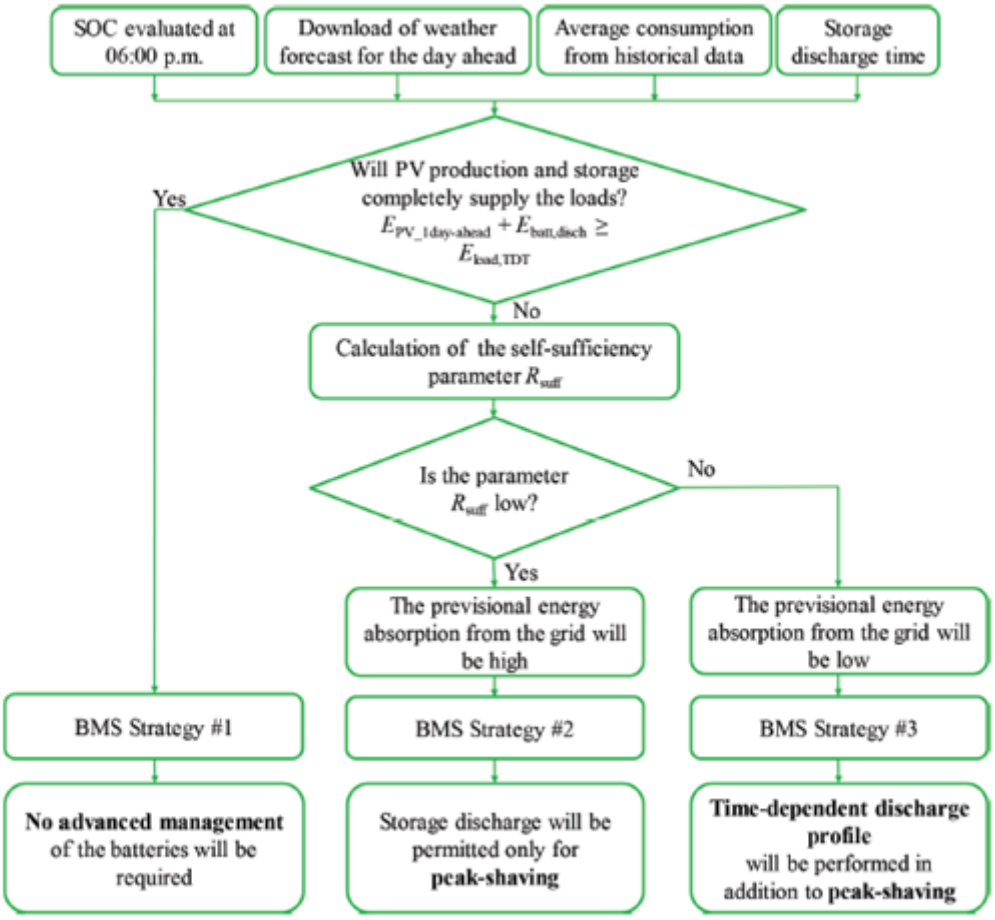

Figure 2.7: Selection of the Strategy to Follow [3].

using appropriate discharge profiles is implemented (BMS3). In cases where there is an excess of energy, meaning that estimated consumption is lower than the combined PV production and storage, intelligent management of the storage system is not necessary (BMS1). Finally, the choice between strategy 2 (BMS2) and strategy 3 (BMS3) is determined by evaluating a parameter known as self-sufficiency [3].

$$R_{suff} = \frac{E_{PV,1day-ahead} + E_{bat,disch}}{E_{load,TDT}}$$

When the ratio R_{suff} falls below a user-defined threshold R_{thres}, Strategy 2 of the Battery Management System (BMS) is implemented. In this strategy, the local generators and storage system contribute a relatively small amount of energy to the loads, while the majority of the energy is supplied by the grid. As a result, there may be high peaks of energy absorption. The energy stored in the batteries is only utilized when the loads exceed a maximum limit $P_{\text{load,max}}$, such as the contracted power absorption limit or another threshold defined by the user [3].
On the other hand, when the ratio R_{suff} is higher than the user-defined threshold R_{thres} but still below one, Strategy 3 of the BMS is employed. This scenario is more favorable than the previous one because a significant portion of the loads is supplied by the photovoltaic (PV) system and storage, leading to a reduced reliance on the grid for energy supply [3].

2.10 Conclusion

In conclusion, the second chapter of our study concentrated on modeling the photovoltaic system and battery storage and laying out the management process for managing battery charge and discharge. We developed techniques based on energy generation, consumption, and storage and deduced mathematical equations for charge voltages. We will present and talk about the simulation findings for battery management in a grid-connected photovoltaic system in the following chapter.

Bibliography

[1] Corne, D., Lones, M.A. (2018). Evolutionary Algorithms. In: Martí, R., Panos, P., Resende, M. (eds) Handbook of Heuristics. Springer, Cham. https://doi.org/10.1007/978-3-319-07153-4_27-1.

[2] Mexis, I., et al. (2020). Battery energy storage systems in the United Kingdom: a review of current state-of-the-art and future applications. Energies, 13(14), 3616. https://doi.org/10.3390/en13143616.

[3] Garniwa, I., Hudaya, C., et al. (2021). Comparison of Battery Models for Battery Energy Storage System Development. Journal of Physics: Conference Series, 1858(1), 012046. https://doi.org/10.1088/1742-6596/1858/1/012046.

[4] Azaroual, M., Ouassaid, M., Maaroufi, M. (2019). Optimal Control for Energy Dispatch of A Smart Grid Tied PV-Wind-Battery Hybrid Power System. 2019 Third International Conference on Intelligent Computing in Data Sciences (ICDS). DOI:10.1109/ICDS47004.2019.8942362.

[5] Chicco, G., Cocina, V., Di Leo, P., Spertino, F. (2014). Weather forecast-based power predictions and experimental results from photovoltaic systems. 2014 International Symposium on Power Electronics, Electrical Drives, Automation and Motion. DOI:10.1109/speedam.2014.6872086.

[6] Muller, M., Marion, B.,Rodriguez, J. (2012). Evaluating the IEC 61215 Ed.3 NMOT procedure against the existing NOCT procedure with PV modules in a side-by-side configuration. 2012 38th IEEE Photovoltaic Specialists Conference. DOI:10.1109/pvsc.2012.6317705.

[7] Bentrar, C., Chaouche, H. (2021). Dimensionnement optimal d'un système énergétique hybride solaire-éolien-batteries utilisant la technique "LPSP" (Master's thesis). [Name of the University or Institution].

[8] Copetti, J. B., Lorenzo, E., & Chenlo, F. (1993). A general battery model for PV system simulation. Progress in Photovoltaics: Research and Applications, 1(4), 283–292. https://doi.org/10.1002/pip.4670010405.

[9] Spertino, F., Ciocia, A., Di Leo, P., Malgaroli, G., & Russo, A. (2019). A Smart Battery Management System for Photovoltaic Plants in Households Based on Raw Production Forecast. Green Energy Advances. https://doi.org/10.5772/intechopen.80562.

[10] Fares, M. M., & Oualid, S. (2022). Gestion de charge/décharge avec mesures de protection d'un banc de batteries dans un système photovoltaïque relié au réseau. Master thesis.

[11] Parthasarathy, K., & Vijayaraj, S. (2020). An Overview of Battery Charging Methods, Charge Controllers, and Design of MPPT Controller based on Adruino Nano for Solar

Renewable Storage Energy System. *INTERNATIONAL JOURNAL OF ENGINEERING RESEARCH & TECHNOLOGY (IJERT)*, 09(11). DOI: 10.17577/IJERTV9IS110214.

Chapter 3

Results and discussion

This chapter presents the simulation results of a sophisticated management technique aimed at optimizing the charging and discharging of batteries in a system connected to the electrical grid. The objective of this technique is to efficiently harness renewable energy sources, specifically photovoltaic and wind, to meet the electrical load requirements of an administrative unit within an Algerian company. The focus of this study is a tertiary housing facility located in the picturesque Tlemcen region. By integrating renewable energy resources into the existing electrical grid, the system aims to reduce dependency on conventional energy sources and minimize the environmental impact associated with electricity generation. The simulation results offer valuable insights into the performance and effectiveness of the management technique, demonstrating its capability to ensure a reliable and sustainable power supply for the administrative unit.The accompanying table 3.1 presents the precise latitude and longitude of the Tlemcen region.

Site	Longitude	Latitude	Altitude (m)
Tlemcen	-1.317 (E)	34.882 (N)	800

Table 3.1: Geographic data of the Tlemcen site [1].

3.1 Simulation parameters

In our study, we aimed to assess the battery charging/discharging management over an extended period, spanning from March 19th at 6 p.m. to March 22nd at 6 a.m. This time frame allowed us to capture the variations in solar irradiance (measured in W/m^2), ambient temperatures [2] (measured in C), and wind speed (measured in m/s) at the site. The data, collected at 5-minute intervals throughout the year 2004 [1], provided valuable insights into the system's performance and energy dynamics.
To facilitate our analysis, we compiled essential technical parameters in various tables. Table (3.2) outlines the specifications of the photovoltaic generator, while Table (3.3) focuses on battery-related parameters. Additionally, Table (3.5) presents the technical details of the wind turbine generator utilized in the system.
During our investigation, we considered several key factors. The nominal power of the photovoltaic generator ($P_{\mathrm{PV,n}} = 18kW$) and the wind power ($P_{\mathrm{WT,n}} = 10kW$) played significant roles in meeting the energy demands of the facility. The battery system consisted of a bank with six parallel branches, each containing fifteen 12 V batteries, resulting in a total nominal battery capacity of $C_{10} = 110Ah$. To address peak consumption periods and mitigate load spikes, we implemented a strategy that limited the maximum power drawn from the grid to

$P_{\text{load, max}} = 8.5kW$. Furthermore, we set the self-sufficiency parameter for power supply, R_{suff}, to be constrained by $R_{lim} = 0.5$. These considerations played a crucial role in evaluating the effectiveness of battery management in renewable energy systems.

Parameter	Designation	Value
γ_{th}	power temperature factor photovoltaic (C)	0.005
η_{cabl}	joule losses	0.99
$\eta_{\text{DC/AC}}$	converter efficiency	0.97
η_{dirt}	losses due to dirt	0.98
η_{mis}	losses due to mismatch	0.97
η_{MPPT}	The efficiency of the maximum power tracker for the PV system	0.99
η_{rfl}	Losses due to reflection	0.97
η_{shad}	Losses due to shading	1.0
$NOCT$	Nominal operating temperature of the cell $(\%C)$	45
G_{NOCT}	Solar irradiance for NOCT conditions $NOCT$ (W/m^2)	800
T_{STC}	Temperature at standard test conditions (C)	25

Table 3.2: The technical parameters of the photovoltaic generator are presented, and the specific numerical values can be verified in article [3] and the associated references.

Parameter	Designation	Value
V_{cell}	Nominal voltage of a battery cell	2.0 V
V_{battery}	Nominal voltage of a battery	12.0 V
$V_{\text{c,limit,max}}$	Maximum allowable charging voltage of a cell	2.45 V
$V_{\text{c,limit,min}}$	Minimum allowable charging voltage of a cell	2 V
$V_{\text{d,limit,min}}$	Minimum allowable discharge voltage of a cell	1.8 V
C_{10}	Nominal capacity of a battery	110 Ah
I_{10}	Nominal current drawn from the battery over a 10-hour period	11 A
SOC_{ini}	Initial state of charge of the batteries	0.9
SOC_{min}	Minimum state of charge	0.5
SOC_{max}	Maximum state of charge	0.95

Table 3.3: The technical parameters of the batteries are provided, and the corresponding numerical values can be cross-verified in article [3] and its referenced sources.

Parameter	Designation	Value
V_{ci}	Start-up wind speed (m/s)	3
V_r	Rated wind speed (m/s)	12
V_{co}	Survival wind speed (m/s)	45

Table 3.4: The technical parameters of the wind turbine generator are presented, and the specific numerical values can be verified in [4] and the associated references.

3.2 Results And discussion

3.2.1 Total discharge time

In Table (3.5), we present the daily values of the total discharge time for the specified site during the month of March 2004. For example, when $TDT = 36$ on March 19th, it signifies that a management strategy spanning 36 hours was chosen, starting from 6 p.m. on the same day and ending at 6 a.m. on March 21st. Similarly, when $TDT = 12$ on March 21st, a 12-hour management strategy was implemented, commencing at 6 p.m. on the same day and concluding at 6 a.m. on March 22nd. Our study involved analyzing the management over a period of 4 days.

Day	$TDT(h)$
1	12
2	12
3	12
4	12
5	12
6	12
7	12
8	12
9	12
10	12
11	12
12	12
13	36
14	12
15	36
16	36
17	36
18	36
19	36
20	36
21	12
22	12
23	12
24	12
25	36
26	12
27	12
28	12
29	12
30	12
31	12

Table 3.5: Daily values of total discharge time for the month of March 2004 on the Tlemcen site.

3.2.2 Strategy 2 for battery charge/discharge management

Based on the current simulation conditions, the assessment of the self-sufficiency parameter (R_{suff}) for the day of March 20th, spanning from 6 a.m. to 6 p.m., yielded a value of 0.36, which falls below the pre-established threshold of $R_{lim} = 0.5$. Consequently, the adoption of strategy 2 for battery charge/discharge management during the period between 6 p.m. on March 19th and 6 a.m. on March 21st is imperative. Notably, strategy 2 entails leveraging the battery charge exclusively to mitigate consumption peaks that surpass $P_{\text{load, max}} = 8.5kW$.

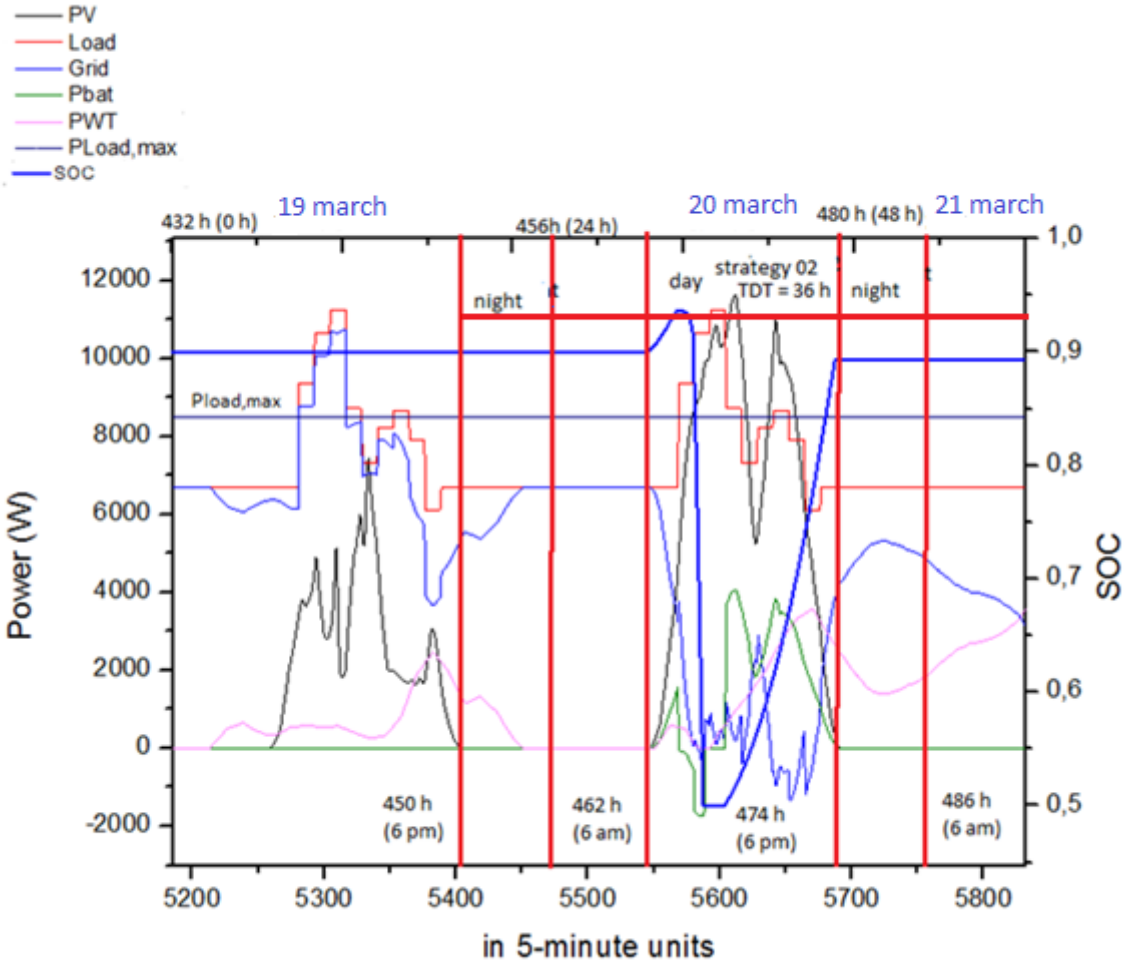

Figure 3.1: The graph displays the power variations (in W) corresponding to the photovoltaic generator, the grid, the batteries, the wind generator, and the electrical load during the period from 6 PM on March 19th to 6 AM on March 21st for strategy 2. Additionally, the graph includes a blue curve representing the battery state of charge as a function of time (in 5-minute intervals).

Figure (3.1) presents a graphical representation of various power values, including photovoltaic power, wind power, battery bank power, grid power, and electrical load, all expressed in watts (W). The figure also displays the state of charge for the storage system at 5-minute intervals during the time period from 6 PM on March 19th to 6 AM on March 21st, with the battery temperature set at $T = 25C$.

Additionally, it should be noted that the initial state of charge (SOC) at the beginning of the study, specifically at 6 PM on March 19th, is considered to be 90% of the nominal capac-

ity. During the initial night of March 19th, an interesting observation is made as depicted in the figure (constant SOC). The batteries remain unchanged in their state of charge, without discharging. This behavior occurs because the power required by the load during that period is lower than the maximum power threshold specified by the user, denoted as $P_{\text{load, max}} = 8.5kW$.

Consequently, the load is supplied by a combination of the grid and the wind power. The power supplied by the grid is determined as $P_{\text{Grid}} = P_{\text{Load}} - P_{\text{WT}}$, where P_{WT} signifies the power generated by the wind turbine. In this particular night, since the photovoltaic power (P_{PV}) is zero, the grid and the wind power sources work together to fulfill the energy demands of the load. On March 20th, during the daylight hours, a significant event takes place.

Starting at 6 am, the batteries begin to charge as the photovoltaic energy becomes available, and the power demand from the load remains below the specified threshold of $P_{\text{load, max}} = 8.5kW$, resulting in no discharge from the batteries. As a consequence, the state of charge (SOC) gradually increases, reaching a value of 0.936 at 464.25 h (8:15 am on March 20th). Throughout this period, the batteries charge at a rate of 1.57 kW.

During this particular moment, the power requirement surpasses the set limit of $P_{\text{load, max}} = 8.5kW$, triggering the discharge of the batteries. As a result, the charging process comes to a halt, and the state of charge undergoes a transition from SOC = 0.936 to $SOC = 0.5$ over a period of 1 hour and 45 minutes.

Meanwhile, the battery bank is capable of supplying electrical power, which can reach a maximum value of 4.034 kW. The discharge process stops once the state of charge reaches its minimum value ($SOC = 0.5$). In such a situation, the power deficit is compensated by the photovoltaic generator, wind generator, and the grid. Additionally, there is an excess of both photovoltaic and wind power available, which can be sold back to the grid.

During this charging period around 11 a.m. on March 20th, the batteries are being charged with a maximum power of 4.076 kW. This charging process continues for a substantial duration of 6 hours and 55 minutes. The extended charging time is made possible due to the integration of the wind generator, which supplies power to the load while ensuring that the load remains below the maximum load threshold of $P_{\text{load, max}} = 8.5kW$. By effectively managing the power distribution, the batteries can maintain a steady charging rate. As a result, the state of charge (SOC) gradually increases and reaches a noteworthy value of 0.89.

During the night of March 21st, the batteries remain uncharged as the power demand from the load remains below the maximum threshold of $P_{\text{load, max}} = 8.5kW$. In this scenario, the load is satisfied by the grid and the wind power, as there is no contribution from the photovoltaic power due to its absence. It is noteworthy that the wind power source plays a significant role in supplying the load during this period.

3.2.3 Charging the batteries during the day on march 21

Since the batteries were not fully charged at the end of the period under strategy 2 (at 6 a.m. on March 21st), we decided to focus on battery charging, taking advantage of the abundance of photovoltaic and wind energy during the day of March 21st, as shown in Figure 3.2. The batteries start charging as soon as the photovoltaic power becomes available at 6 a.m. on March 21st (486 hours into the simulation).

The state of charge (SOC) begins at a value of $SOC = 0.89$ and reaches $SOC = 0.95$ at 489 hours and 10 minutes (9:10 a.m. on March 21st), maintaining this value until the end of the day (6 p.m. on March 21st). The power delivered to the batteries (positive value) reaches a maximum of 5.028 kW. The load is entirely satisfied by the combination of photovoltaic and wind power, with any deficiencies being supplemented by the grid. As there is an abundance of photovoltaic power and sufficient wind power on this particular day, a portion of the surplus energy is sold back to the grid, resulting in a negative value for grid power.

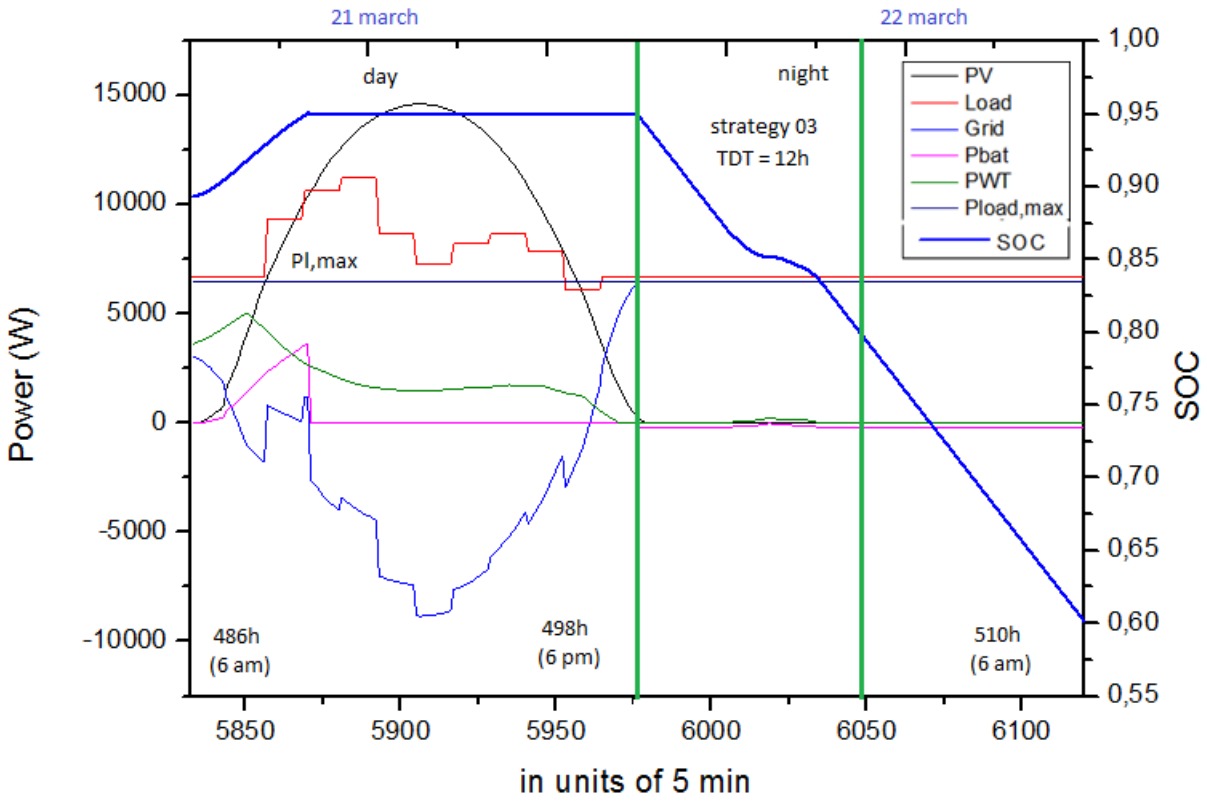

Figure 3.2: Power Variation and Battery State of Charge (SOC) for Photovoltaic, Wind, Grid, Batteries, and Load during March 21st to March 22nd: Strategy 3.

3.2.4 Strategy 3 for battery charge/discharge management

The calculated value of the self-sufficiency parameter R_{suff} for the time period from 6 p.m. on March 21st to 6 a.m. on March 22nd is found to be 0.95. This value exceeds the predetermined threshold of $R_{\text{lim}} = 0.5$ and falls below 1, indicating a satisfactory level of self-sufficiency.

As a result, it is recommended to implement strategy 3 for battery charge/discharge management, which involves employing a time-dependent discharge profile and addressing consumption peaks. However, upon analyzing Figure 3.2, it becomes apparent that the electrical load during this period does not exhibit significant consumption peaks, and the power demand remains below the maximum limit of $P_{\text{load, max}} = 8.5kW$. Consequently, in order to utilize strategy 3 for battery discharge, the maximum charging power has been adjusted to $P_{\text{load, max}} = 6.45kW$.On the other hand, The discharge current I_d is given by:

$$I = \frac{P_{\text{l}} - P_{\text{WT}} - P_{\text{load, max}}}{\eta_{\text{inv}} V_{\text{l, nominal}}} \tag{3.1}$$

In the equation, P_{l} represents the power of the load, $P_{\mathrm{load,\ max}}$ refers to the maximum power of the load, η_{inv} represents the efficiency of the inverter, and $V_{\mathrm{l,\ nominal}}$ denotes the nominal voltage of the load (AC).
During the night of March 22nd, the batteries play a crucial role in ensuring a seamless power supply during the hours of darkness. With a starting state of charge (SOC) of 0.95 at 6 PM on March 21st, they embark on a steady discharge, gradually delivering power to meet the nighttime energy demands. By 6 AM on March 22nd, their diligent efforts result in an SOC of 0.6, showcasing their ability to sustain reliable power availability throughout the night.

Although the power output during this period may be relatively low, at 208W, it highlights the batteries' contribution to maintaining a stable and continuous energy flow.

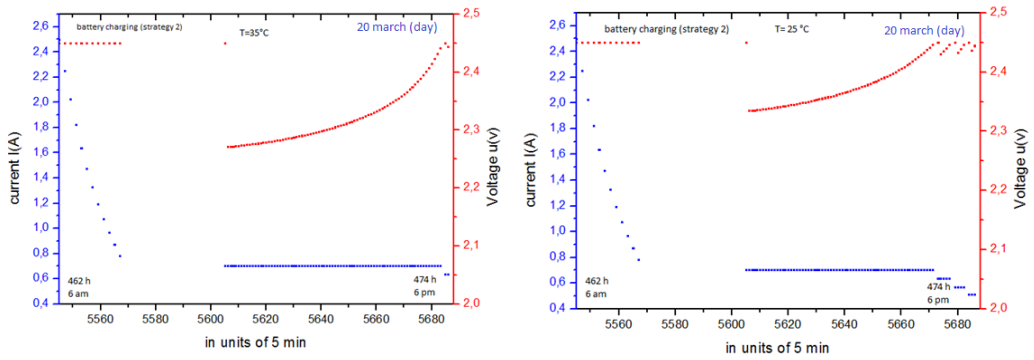

Figure 3.3: Variation of the voltage of a battery cell and the charging current for the strategy 2 and this for two battery temperatures: at $T = 25C$, at $T = 35C$.

The graph (Figure 3.3) illustrates the variations in voltage and charging current for a battery cell under Strategy 2 at two different temperatures. At a temperature of $T = 25C$, the charging process begins on March 20th at 6 AM, with a constant charging voltage of 2.45V. However, the charging current exhibits a range of fluctuations, starting at 2.5A and gradually decreasing to 0.78A over a period of 1 hour and 50 minutes.
Subsequently, a second variation in voltage occurs, spanning 5 hours and 35 minutes, where the voltage ranges from 2.33V to 2.446V, while the charging current remains constant at 0.7A. This phase highlights the stability of the charging current while the voltage undergoes moderate fluctuations.

Another interesting observation is a brief period of 20 minutes, during which the voltage remains constant at 2.43V, while the current remains stable at 0.64A. This period demonstrates the battery ability to maintain a consistent voltage output, despite minor variations in the current. Similarly, there is a subsequent 15-minute period in which the voltage ranges from 2.45V to 2.43V, while the current remains constant at 0.57A. This phase further emphasizes the battery ability to maintain a stable current while experiencing slight voltage variations.

Lastly, there is a voltage variation from 2.45V to 2.43V, accompanied by a constant current of 0.514A. This final segment showcases the battery ability to sustain a steady current output, even when the voltage undergoes slight fluctuations. Overall, the graph provides valuable insights into the behavior of the battery cell under Strategy 2 at different temperatures.

The observations suggest that the battery demonstrates stable voltage and current performance, with varying degrees of fluctuations depending on the specific phase of the charging

process. These findings contribute to our understanding of battery behavior and can be utilized in optimizing charging strategies for enhanced battery performance and longevity.

The subsequent simulation was conducted (Figure 3.3 the graph on the left) at a higher temperature of $35C$, yielding interesting results regarding the voltage and current behavior of the battery cell. Initially, the voltage remains constant at 2.45V, while the charging current exhibits a range of fluctuations, varying from 2.5A to 0.7A over a period of 1 hour and 50 minutes.

This observation suggests that the battery voltage remains stable despite significant changes in the charging current, indicating its resilience in adapting to different temperature conditions. Following this, there is a notable voltage variation ranging from 2.27V to 2.44V, while the charging current remains constant at 0.7A over a period of 6 hours and 40 minutes.

This finding demonstrates the battery's ability to maintain a steady current output despite fluctuations in the voltage, which is particularly significant given the higher temperature of $35C$. Lastly, during a 15-minute period, the voltage undergoes a minor variation from 2.45V to 2.44V, while the current remains constant at 0.64A.

This observation highlights the battery's capability to sustain a consistent current output, even when experiencing slight voltage fluctuations at elevated temperatures. Comparing these results to the previous simulation at $T = 25C$, it becomes evident that the higher temperature has an impact on the battery's behavior. Despite the voltage remaining constant at 2.45V in both cases, the charging currents differ, emphasizing the temperature-dependent characteristics of the battery's performance. The provided information further expands our understanding of the battery's behavior under varying temperature conditions.

On the other hand, Figure 3.4 provides valuable information regarding the temporal behavior of voltage and charging current for a battery cell on March 21st. The analysis considers Strategy 3 and examines two distinct battery temperatures: $T = 25C$ and $T = 35C$.

Throughout the observation period, the charging voltages span a range of 2.42V to 2.45V, with the highest recorded voltage being 2.45V. Likewise, the charging current reaches its maximum value at 2.5A and can descend to a minimum of 0.23A.

For the battery temperature of $T = 25C$ (shown in the left figure), the charging process initiates at 6 am on March 21st with a steady voltage of 2.45V. Concurrently, the charging current experiences a gradual decline from an initial value of 2.5A. Throughout the charging cycle, the voltage steadily increases, indicating the accumulation of charge within the battery.

Notably, the charging periods follow one another with successive plateaus of decreasing current levels. In the final stage of charging, the current diminishes to 0A while the voltage remains at 2.45V, indicating that the battery ceases to charge due to reaching a state of 95% State of Charge (SOC).On the other hand, the right figure of the same graph depicts the variation in voltage and charging current for Strategy 3 at a higher battery temperature of $T = 35C$.

In comparison to the $T = 25C$ scenario, the charging current experiences a slightly more rapid decline. Moreover, the charging voltage exhibits a more pronounced increase throughout the charging process when the battery temperature is elevated to $T = 35C$.These observations highlight the impact of battery temperature on the charging behavior. At a higher temperature, the charging current tends to drop more quickly, and the charging voltage shows a more significant increase. These findings emphasize the importance of considering battery temperature in

optimizing charging strategies to enhance battery performance and longevity.

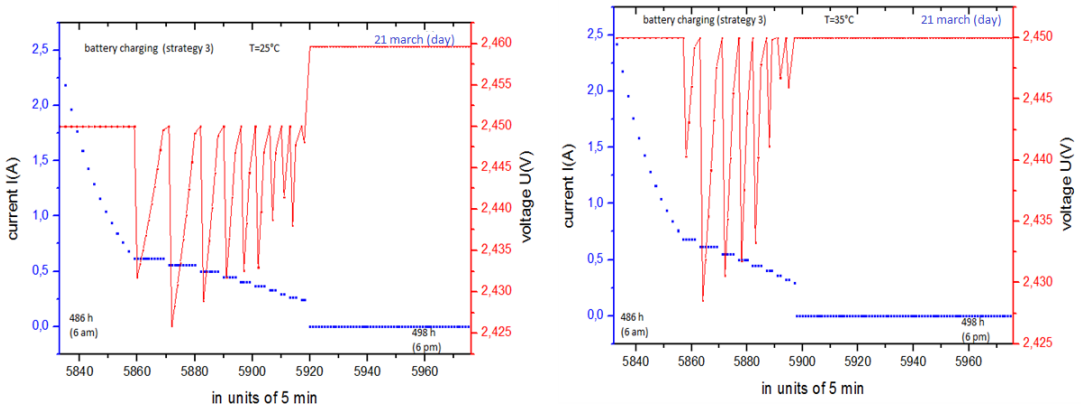

Figure 3.4: Variation of the voltage of a battery cell and the charging current for strategy 3, considering two battery temperatures: at $T = 25C$, at $T = 35C$.

The Figure (3.5) illustrates the variation in voltage and discharge current of a battery cell for Strategy 2, considering two different battery temperatures: $T = 25C$ and $T = 35C$.

For a temperature of $25C$, the voltage ranges from 2.015V to 1.87V, while the current varies between 0.27A and 0.934A. Subsequently, the voltage stabilizes at a constant value of 1.8V, accompanied by a current ranging from 1.5A to 10.78A. Finally, the voltage remains constant at 1.8V, and the current is consistently 0A. This means that in the last stage, the battery is fully discharged, and no current flows in or out of the cell.

Similarly, at a temperature of $T = 35C$, the voltage varies from 2.01V to 1.86V, and the current ranges from 0.27A to 0.93A. As before, the voltage stabilizes at 1.8V, while the current varies from 1.5A to 10.78A. In the final stage, both the voltage and the current remain constant at 1.8V and 0A, respectively. Here, the current being 0A indicates that the battery is completely discharged and no longer supplying any electrical current.

The observation of a current value of 0A at the end of the discharge process is significant, as it indicates that the battery has reached its minimum charge level and cannot deliver any more current. This information is essential for understanding the battery behavior under Strategy 2 and its discharge characteristics at different temperatures. Additionally, it provides valuable insights into the battery performance and can help optimize the battery usage and management strategies.

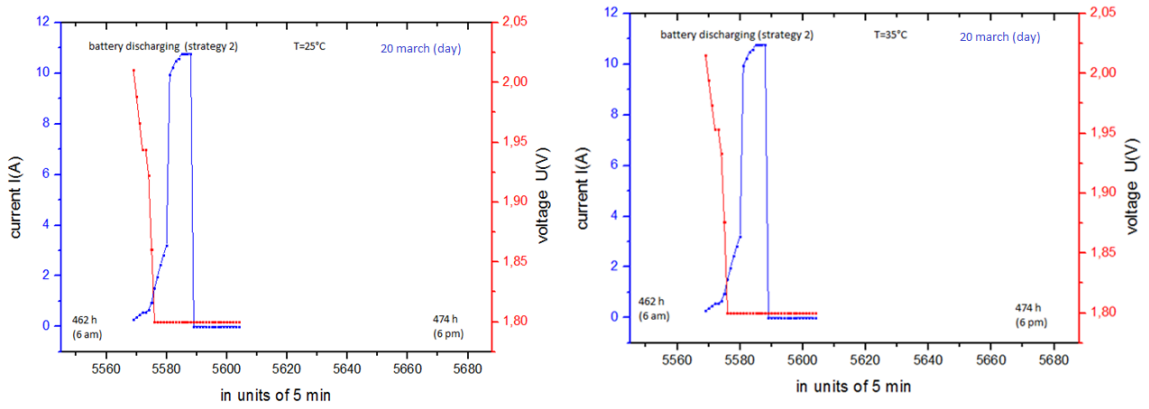

Figure 3.5: Variation in voltage of a battery cell and discharge current for Strategy 2, considering two battery temperatures: at $T = 25C$, at $T = 35C$.

Figure 3.6 depicting the variation in voltage and discharge current for Strategy 3, considering battery temperatures of $25C$ and $35C$, offers a comprehensive understanding of the battery cell behavior. At a temperature of $25C$, the voltage remains constant at 1.8V, which suggests a stable and controlled discharge process. Simultaneously, the current maintains a consistent value of 1.288A, indicating a steady discharge rate.

Upon closer examination, the voltage undergoes two significant variations. Initially, it ranges from 1.82V to 2.049V, accompanied by a corresponding current range of 1.098A to 0.088A. This change in voltage suggests a shift in the battery internal resistance and capacity. Subsequently, the voltage fluctuates from 2.033V to 1.8V, while the current ranges from 0.151A to 1.224A. This behavior could be attributed to the battery reaching a lower state of charge, resulting in a decrease in available capacity.

For the temperature of 35°C, the voltage experiences a slight variation from 1.812V to 1.803V, maintaining relative stability. Similarly, the current remains constant at 1.288A, indicating a consistent discharge rate. This behavior could be attributed to the thermal effects on the battery's internal resistance and the balance between electrochemical reactions.

Notably, the second voltage variation occurs from 1.83V to 2.051V, accompanied by a current range of 1.098A to 0.088A. This behavior suggests a combination of thermal effects and changes in the battery capacity and internal resistance due to discharge. Subsequently, the voltage varies from 2.036V to 1.811V, while the current ranges from 0.151A to 1.225A. These fluctuations could be attributed to the dynamics of the electrochemical processes within the battery during discharge.

Ultimately, both temperature scenarios converge with the voltage stabilizing at 1.8V, indicating a discharge termination point. Simultaneously, the current remains constant at 1.288A, representing a steady-state condition.

In summary, the provided figure offers valuable insights into the behavior of the battery cell under Strategy 3 at different temperatures. The observed voltage variations reflect changes in the battery's internal resistance, capacity, and state of charge, influenced by temperature effects. Understanding these dynamics is crucial for developing effective battery management strategies, optimizing performance, and ensuring safe and reliable operation in various temperature environments.

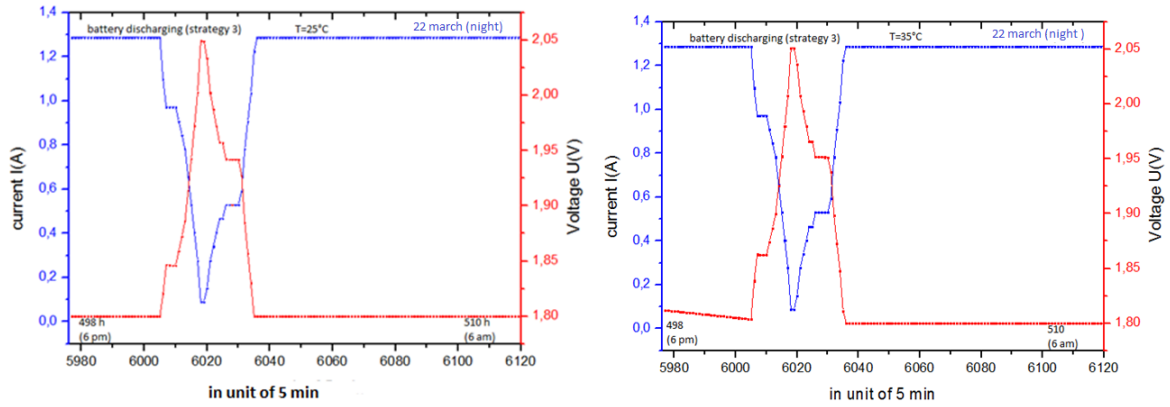

Figure 3.6: Variation in voltage of a battery cell and discharge current for Strategy 3, considering two battery temperatures: at $T = 25C$, at $T = 35C$.

3.2.5 New strategy

3.2.5.1 Total discharge time

In this table , we present the daily values of the total discharge time for the specified site during the month of March 2004.

day	TDT (h)
1	36
2	36
3	12
4	12
5	12
6	36
7	12
8	12
9	36
10	12
11	12
12	12
13	36
14	36
15	36
16	36
17	36
18	36
19	36
20	36
21	12
22	12
23	36
24	12
25	36
26	36
27	12
28	36
29	12
30	36
31	12

Table 3.6: Daily values of total discharge time for the month of March 2004 on the Tlemcen site .

In this strategy, two key parameters are considered: the maximum load power (P_{load_max}) and the maximum photovoltaic power (P_{PV_max}). The value of P_{load_max} is set at 6450 W, indicating the load level above which the system will enter the discharging phase.

On the other hand, P_{PV_max} is defined as 5500 W, representing the PV power level above which the system will prioritize charging. When both P_{load_max} and P_{PV_max} are reached simultaneously, the system gives priority to charging. This means that if the load power is below P_{load_max} and the PV power exceeds P_{PV_max}, the excess power will be utilized to charge the battery.

Additionally, the initial charge current is set at 5A, determining the rate at which the battery is initially charged.Lastly, the parameter T_{cell} is specified as $35C$, indicating the temperature at which the battery cell operates.

3.2.5.2 battery charge/discharge management

In the graph (3.7) representing the events of day 2 in March, we observe the behavior of the battery throughout the day. At 6 am, the load surpasses the predetermined threshold of P_{load_max}, causing the battery to initiate the discharging process. As a result, the battery begins providing power to meet the demand from the electrical load.

However, the situation changes later in the day as the photovoltaic power generated exceeds the predefined limit of P_{PV_max}. This surplus of power from the photovoltaic panels prompts a shift in the battery's operation. Instead of discharging, the battery seizes the opportunity to replenish its energy reserves. It starts charging using a portion of the excess power generated by the photovoltaic panels.

This charging phase continues until the photovoltaic power drops below the threshold of P_{PV_max}. At this point, the battery reverts to discharging again to fulfill the energy requirements of the electrical load, as the load still exceeds the predefined limit of P_{load_max}.

This cycle of alternating between charging and discharging continues throughout the day, driven by the interplay between the load, photovoltaic power, and the predetermined thresholds. Eventually, the battery's state of charge reaches the desired level of 50 percent. The graph captures these fluctuations and showcases the dynamic behavior of the battery as it balances between discharging, charging, and reaching specific state of charge targets.

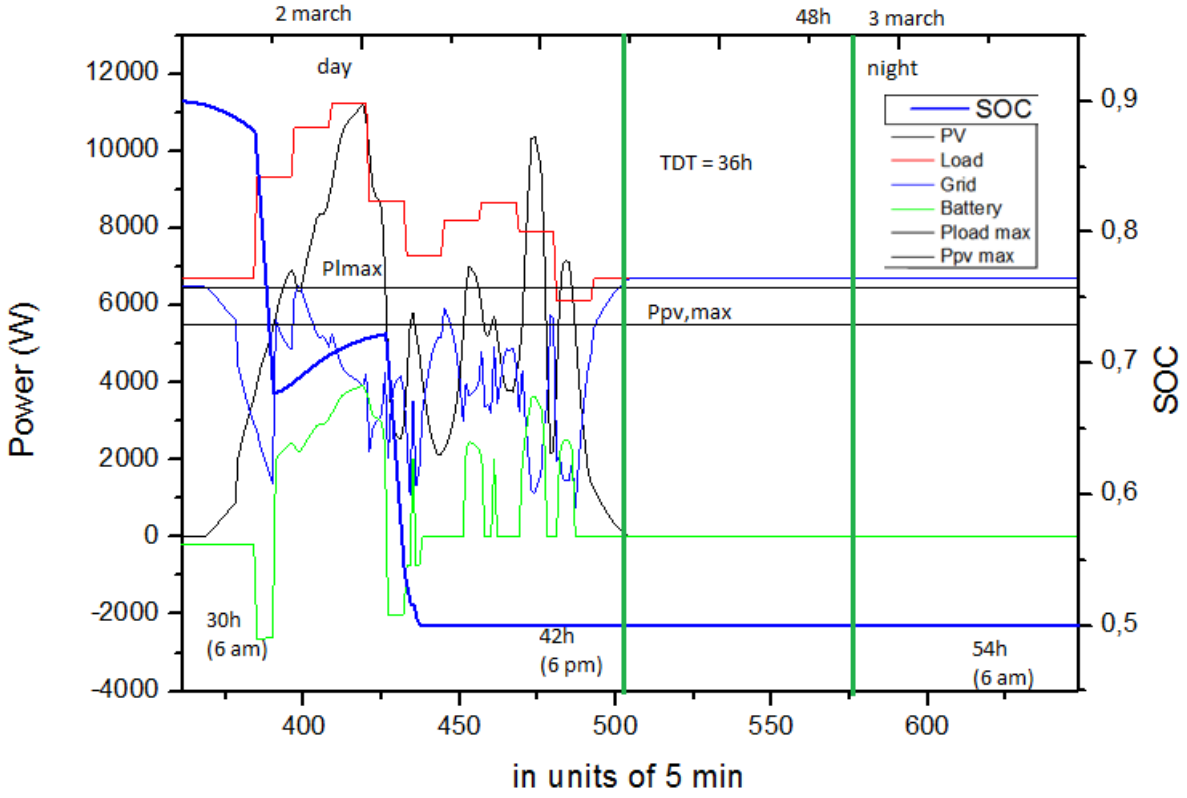

Figure 3.7: Power Variation and Battery State of Charge (SOC) for Photovoltaic, Wind, Grid, Batteries, and Load during March 2nd .

When examining the voltage and current behavior of the battery 3.7 , we can observe distinct patterns. Initially, during the discharge phase, the battery operates at a relatively low

current of 1 ampere, corresponding to a voltage of 2 volts. The discharge occurs gradually as the load draws power from the battery.

However, there is a notable shift in consumption, leading to a significant increase in discharge current. The current rises to 14.5 amps, accompanied by a slight decrease in voltage. This surge in current indicates a higher power demand from the load, resulting in a more rapid discharge of the battery's stored energy.

As the photovoltaic (PV) power rises and exceeds the predefined threshold of P_{PV_max}, the battery transitions from discharging to charging mode. In this transition, the current experiences a rapid increase, quickly reaching 5 amps. Consequently, the voltage also jumps to its upper limit of 2.26 volts. The charging process initiates, and the current starts to decrease gradually.

During the charging phase, the battery harnesses the surplus power from the PV panels to replenish its energy reserves. As the PV power drops below P_{PV_max}, signaling the end of the charging opportunity, the battery resumes discharging. It continues to provide power until the state of charge reaches the desired level of 50 percent.

Overall, the graph illustrates the dynamic nature of the battery's voltage and current characteristics as it adapts to changing load and PV power conditions, switching between discharging and charging modes accordingly to meet energy demands and maintain the desired state of charge.

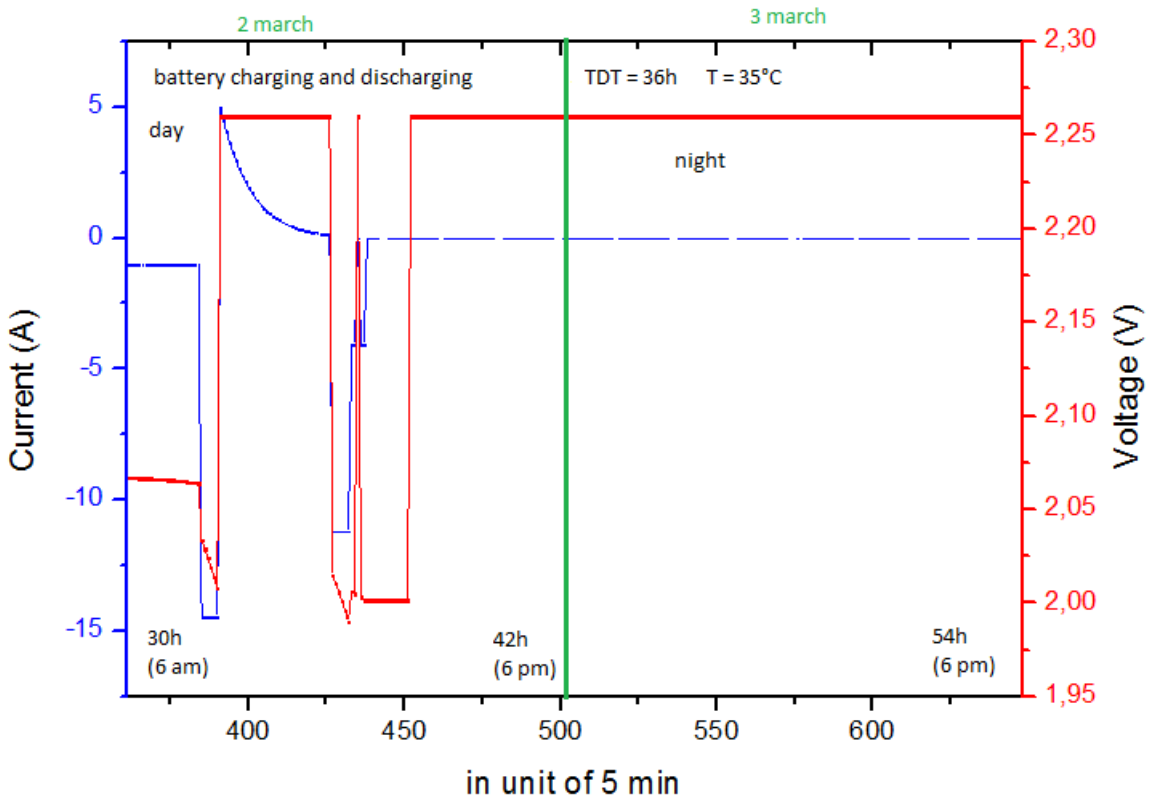

Figure 3.8: Variation of the voltage of a battery cell and discharge and charge current , considering battery temperatures at $T = 35C$.

3.3 Conclusion

During the analysis conducted in this study, the battery management system for a hybrid/wind/photovoltaic system was examined. The simulation results provided valuable insights into the performance of two different strategies: Strategy 2 and Strategy 3. Strategy 2 involved discharging the batteries only during peak consumption periods, while Strategy 3 aimed to reduce grid dependency by discharging the batteries during consumption peaks and at night.

Initially, Strategy 2 was chosen based on the TDT value of 36 hours, indicating that the batteries could meet the system's power requirements for one day and two nights. This strategy effectively utilized grid power during the night, allowing the batteries to remain fully charged. However, on March 21st at 6 pm, the TDT decreased to 12 hours, necessitating a reevaluation of the system's operation.

Upon analyzing the parameter Rsuff, Strategy 3 was deemed more suitable for this period. This strategy facilitated the discharge of the batteries during consumption peaks and at night, thereby reducing reliance on grid power. By utilizing discharge profiles based on time, the system optimized the utilization of stored energy and minimized grid absorption. Additionally, surplus energy generated by the photovoltaic and wind turbine generators could be sold back to the grid once the batteries reached their full capacity.

The implementation of an intelligent battery management system, ensured the system's efficient operation. This study demonstrated the potential for reducing grid dependency, enhancing self-sustainability, and optimizing the utilization of renewable energy sources in a hybrid/wind/photovoltaic system with battery storage.

In conclusion, the results obtained from this research provide valuable insights into the effectiveness of different strategies for battery management in a hybrid/wind/photovoltaic system. By employing Strategy 3, which focuses on discharging the batteries during consumption peaks and at night, the system can minimize reliance on the grid and maximize the utilization of renewable energy sources. These findings contribute to the advancement of sustainable energy systems and highlight the importance of intelligent battery management for optimizing system performance and reducing environmental impact.

Bibliography

[1] Helioclim-3 Archives for Free. (2022, June). Retrieved from http://www.soda-pro.com/web-services/radiation/helioclim-3-archives-for-free

[2] Bentrar, M., & Chaouche, H. (2021). Dimensionnement optimal d'un système énergétique hybride solaire-éolien-batteries utilisant la technique LPSP. Mémoire d'ingénieur, ESSA-Tlemcen.

[3] Spertino, F., Ciocia, A., Di Leo, P., Malgaroli, G., & Russo, A. (2019). A Smart Battery Management System for Photovoltaic Plants in Households Based on Raw Production Forecast. *Green Energy Advances*. doi:10.5772/intechopen.80562.

[4] Ding Energy. (n.d.). 10kW Horizontal Axis Wind Turbine. Retrieved from https://ding-energy.store/products/10kw-horizontal-axis-wind-turbine.

General conclusion

In conclusion, this thesis has focused on the development and implementation of an advanced battery management system for a hybrid/wind/photovoltaic system. The primary objective was to optimize the charge/discharge management of batteries and ensure their protection within the system. Through extensive simulation studies and analysis, several key findings and outcomes have been obtained. Firstly, the evaluation of different battery management strategies, namely Strategy 2 and Strategy 3, provided valuable insights into their effectiveness in balancing power supply and demand. Strategy 2, which prioritizes discharging the batteries only during peak consumption periods, proved to be suitable when the Time of Day Threshold (TDT) exceeded a certain duration. On the other hand, Strategy 3, which involves discharging the batteries during consumption peaks and at night, was more appropriate when the TDT decreased.

Furthermore, the integration of wind turbines into the system was explored, not only for power generation but also for load supply. This integration enhanced the system's overall reliability and reduced reliance on the grid during periods of low photovoltaic generation. The findings demonstrated the potential benefits of utilizing multiple renewable energy sources to improve system performance and reduce environmental impact.

The proposed battery management system successfully optimized the use of renewable energy sources, reduced grid dependency, and ensured efficient utilization of the batteries. By monitoring and controlling the batteries' operation, the system achieved optimal charge/discharge rates, thereby prolonging their lifespan and maximizing their performance.

Moreover, the protective measures implemented within the battery management system played a crucial role in safeguarding the batteries from adverse operating conditions. Overall, this research contributes to the field of renewable energy systems by providing practical solutions for efficient battery management in hybrid/wind/photovoltaic systems. The developed battery management system optimizes power utilization, enhances system reliability, and promotes sustainability by minimizing reliance on traditional energy sources.

The outcomes of this thesis have implications for the wider adoption and implementation of hybrid renewable energy systems. The knowledge gained from this research can guide the development of more advanced and efficient battery management systems, leading to the establishment of sustainable energy systems that reduce greenhouse gas emissions and mitigate climate change.

In conclusion, the findings presented in this thesis provide valuable insights and practical recommendations for the design, implementation, and management of battery systems in hybrid/wind/photovoltaic systems. The research outcomes contribute to the advancement of renewable energy technologies and pave the way for a greener and more sustainable future.